

Practical Systems Biology

Peter S. Swain

`peter.swain@ed.ac.uk`

Biological Sciences, University of Edinburgh

Contents

1	Overview	3
2	Modelling biochemical reactions	4
2.1	Chemical rate equations	4
2.1.1	Example: dimerisation	5
2.1.2	Rates of first-order reactions	6
2.1.3	Diffusion-limited reactions	7
2.1.4	The concentration of one molecule	7
2.2	Equilibrium and detailed balance	8
2.2.1	Finding concentrations at equilibrium	8
2.3	The law of mass action	9
2.4	Modelling signal transduction I	9
2.5	Thermodynamic cycles	11
2.6	Ultrasensitivity and the Hill number	12
2.7	Describing response curves	14
2.7.1	Sensitivity	14
2.8	Modelling signal transduction II	15
2.9	Allostery – and the Monod-Wyman-Changeux model – as a means to generate ultrasensitivity	15
2.9.1	Allosteric molecules with a single binding site for a regulator	16
2.9.2	Allosteric molecules with two binding sites for regulators	17
2.9.3	Allosteric molecules with n binding sites for regulators	19
2.9.4	Limits of the Monod-Wyman-Changeux equation	20
2.10	Modelling signal transduction III	21
2.11	Enzyme kinetics	22
2.12	Modelling signal transduction IV	24
2.13	Enzymatic cascades	25
2.14	Zero-order ultrasensitivity	26
2.15	Summary	27

3	Modelling gene expression	28
3.1	Modelling constitutive expression	28
3.1.1	Modelling transcription	29
3.1.2	Modelling translation	29
3.2	Repression by a single repressor	30
3.3	Activation by a single activator	31
3.4	Activation by two activators	32
3.4.1	Multiple transcriptionally active states	34
3.5	General regulation	34
3.6	Including non-specific binding to DNA	35
3.7	Modelling signal transduction V	37
4	Positive feedback and bistability	38
4.1	MAP kinase cascades: a one dimensional example	38
4.2	Bifurcation diagrams and hysteresis	40
4.3	A genetic switch: a two dimensional example of a saddle-node bifurcation	41
5	Negative feedback and oscillations	46
5.1	Degradation stabilises molecular numbers	46
5.2	Negative feedback is stabilising	46
5.3	Delayed negative feedback can cause oscillations	47
5.4	Circadian rhythms	47
5.4.1	Competitive inhibition	48
5.4.2	The Tyson <i>et al.</i> model	50
5.4.3	Dimerisation	50
5.4.4	The final model with two rate equations	51
5.5	Relaxation oscillations	52
5.6	Oscillations through both positive and negative feedback	52
5.6.1	Understanding a dual feedback oscillator	53
	Appendix A Simulating stochastic biochemical reactions	58
A.1	Mesoscopic and macroscopic rates	59
	Appendix B Fitting data	59

1 Overview

These notes from the basis of lectures given to MSc students in the School of Biological Sciences at the University of Edinburgh.

In Sections 2 and 3, we start with the fundamentals of mathematical modelling, both of signal transduction and of gene expression. These sections are necessarily the most complex mathematically, but throughout we will illustrate the techniques by developing a model of a signalling pathway (Fig. 1). We then turn to the effects of positive and negative feedback. Positive feedback can generate bistability and is used by cells to differentiate irreversibly (Sec. 4). Negative feedback can cause oscillations and drives biological rhythms (Sec. 5).

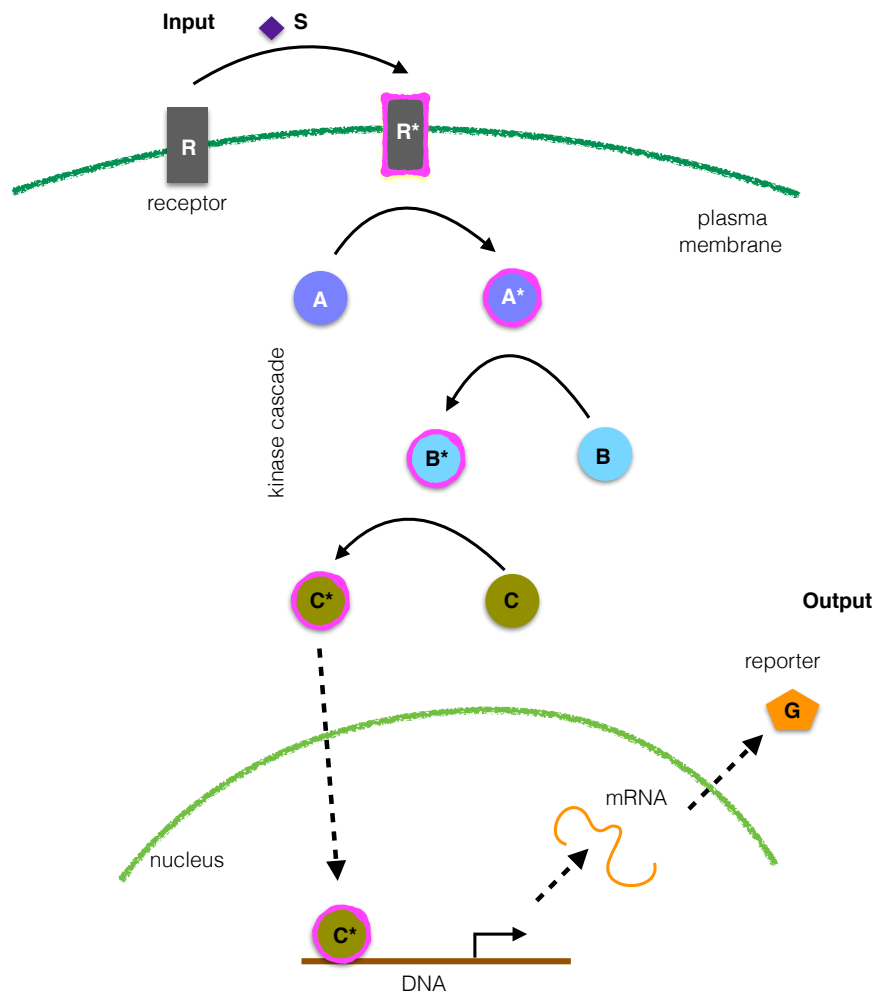
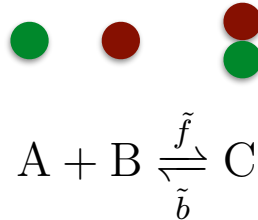


Figure 1: An idealised model of a eukaryotic signalling pathway: an input, ligand S , activates receptors at the plasma membrane — activation is shown in purple, which in turn activate a cascade of kinases. The last kinase in the cascade, C , enters the nucleus once activated and enables expression of a reporter gene. The protein produced by this gene, G , is the system's output.

2 Modelling biochemical reactions

2.1 Chemical rate equations

Consider two reactions: the first occurs when an A and a B molecule come together, react, and form a C molecule; the second occurs when a C molecule dissociates back into an A and a B molecule. For example, the A molecule could be a receptor on the cell membrane and the B molecule could be an extracellular ligand. These two molecules come together reversibly to form a receptor-ligand complex, C , which can signal intracellularly. Let the rate at which a pair of A and B molecules associate into a C molecule be \tilde{f} (measured in inverse seconds) and the rate at which a C molecule dissociates be \tilde{b} (also measured in inverse seconds), then:



The association rate, \tilde{f} , is determined by two times: the time taken by a molecule of A and a molecule of B to find each other by diffusion, t_{diff} , and the time taken for the two molecules to react once in physical proximity, t_{reac} . We can write

$$\text{time of reaction} = t_{\text{diff}} + t_{\text{reac}} \quad (2.1)$$

and so the association rate, which is inversely related to the time of the reaction, obeys

$$\tilde{f} = (t_{\text{diff}} + t_{\text{reac}})^{-1}. \quad (2.2)$$

The dissociation rate, \tilde{b} , is determined by one time — the half-life of the molecule C :

$$\tilde{b} = \frac{\log 2}{\text{half-life of } C}. \quad (2.3)$$

We wish to describe how the number of C molecules, N_C , changes with time. Over a small interval of time dt , the association and dissociation reactions will both occur (we will include stochastic effects later). The number of pairs of A and B molecules is $N_A N_B$, and $\tilde{f} dt N_A N_B$ of these pairs will associate over a time dt . The number of C molecules that dissociate over dt is $\tilde{b} dt N_C$. Therefore, the number of C molecules at a time $t + dt$ is the number of C molecules at time t plus the number gained in association reactions and minus the number lost in dissociation reactions:

$$N_C(t + dt) = N_C(t) + \tilde{f} dt N_A N_B - \tilde{b} dt N_C \quad (2.4)$$

or

$$\frac{N_C(t + dt) - N_C(t)}{dt} = \tilde{f} N_A N_B - \tilde{b} N_C. \quad (2.5)$$

Taking the limit of dt going to zero, we have

$$\frac{dN_C}{dt} = \tilde{f} N_A N_B - \tilde{b} N_C \quad (2.6)$$

which is an example of a chemical rate equation.

Chemical rate equations are usually written in terms of concentrations, which we measure in molar units – the number of moles of a substance per litre. Let $[C]$ denote the molar concentration of C , then

$$[C] = \frac{N_C}{n_A V} \quad (2.7)$$

where $n_A \simeq 6.02 \times 10^{23}$ is Avogadro's number and V is the volume of the cell in litres. To convert Eq. 2.6 into an equation for the rate of change of the concentration of C , we must divide Eq. 2.6 by $n_A V$. This division gives

$$\frac{d}{dt} \cdot \frac{N_C}{n_A V} = \tilde{f} \frac{N_A}{n_a V} \cdot \frac{N_B}{n_a V} n_a V - \tilde{b} \frac{N_C}{n_A V} \quad (2.8)$$

and so

$$\frac{d[C]}{dt} = \tilde{f} n_A V [A][B] - \tilde{b} [C] \quad (2.9)$$

where $[A]$ is the concentration of A and $[B]$ is the concentration of B .

If we define macroscopic reactions rates, or rates for reactions involving concentrations, as

$$\begin{aligned} f &= \tilde{f} n_A V \\ b &= \tilde{b} \end{aligned} \quad (2.10)$$

then

$$\frac{d[C]}{dt} = f[A][B] - b[C]. \quad (2.11)$$

The units of the macroscopic association rate f are $\text{M}^{-1} \text{s}^{-1}$. This rate should not change with volume because molecular species are now measured in concentrations. The rate of association of a pair of molecules, \tilde{f} , does, however, depend on volume and will decrease in larger volumes because it is more difficult for molecules to find each other [1]. The volume-dependence in Eq. 2.10 cancels out the volume-dependence of \tilde{f} . In contrast, the units of the macroscopic rate b do not change, remaining s^{-1} , because b describes a dissociation reaction that depends principally on the chemical species involved and occurs at a rate independent of volume.

2.1.1 Example: dimerisation

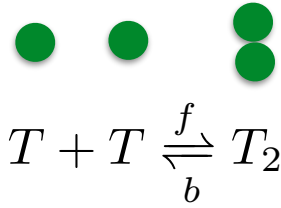
Many membrane receptors reversibly dimerise to form a receptor-receptor dimer, and transcription factors in bacteria often dimerise before binding to DNA, but the dimerisation reaction is unusual.

Let T denote a transcription factor and T_2 denote a dimer of two transcription factors. These species satisfy the reaction $2T \rightleftharpoons T_2$. The rate equations for this system are atypical because the f reaction removes two molecules of T rather than one and the b reaction releases two molecules. Although the association reaction proceeds at the rate $f[T]^2$ and the dissociation reaction proceeds at the rate $b[T_2]$, we now have

$$\frac{d[T]}{dt} = -2f[T]^2 + 2b[T_2] \quad (2.12)$$

because the number of T molecules changes by two for both reactions. The dimer, T_2 , obeys

$$\frac{d[T_2]}{dt} = f[T]^2 - b[T_2] \quad (2.13)$$



because only one molecule of dimer either forms or dissociates.

Summing Eq. 2.12 and twice Eq. 2.13 gives

$$\frac{d[T]}{dt} + 2\frac{d[T_2]}{dt} = 0 \quad (2.14)$$

implying that

$$[T] + 2[T_2] = \text{constant} = [T]_0 + 2[T_2]_0 \quad (2.15)$$

where $[T]_0$ is the initial concentration of monomers and $[T_2]_0$ is the initial concentration of dimers.

The dimerisation reaction only changes the form of T molecules, either from monomers to dimers or vice versa, and does not lead to either their synthesis or destruction. Consequently, the number of T molecules is conserved and determined by the initial numbers of monomers and dimers. The conservation law, Eq. 2.15, reflects that a dimer contains twice as many T molecules as a monomer.

2.1.2 Rates of first-order reactions

In Eq. 2.3, there is a $\log 2$ term. This term comes from the definition of half-life: the average time taken for the number, and so also typically the concentration, of molecules to halve. If a molecule degrades at a rate k , then the number of molecules N obeys

$$\frac{dN}{dt} = -kN. \quad (2.16)$$

If we have N_0 molecules initially, Eq. 2.16 has the solution

$$N = N_0 e^{-kt}, \quad (2.17)$$

and the number of molecules decreases exponentially with time.

To determine the molecule's half-life, we should re-write this solution in powers of 2. Using the mathematical relation for any variable a

$$\begin{aligned} e^a &= (e^{\log 2})^{\frac{a}{\log 2}} \\ &= 2^{\frac{a}{\log 2}} \end{aligned}$$

we can write Eq. 2.17 as

$$N = N_0 2^{-\frac{kt}{\log 2}}. \quad (2.18)$$

After a period of time equal to the half-life, $t_{\frac{1}{2}}$, has passed, the number of molecules will be, by definition, $N_0/2$. Therefore Eq. 2.18 implies

$$N_0 2^{-1} = N_0 2^{-kt_{\frac{1}{2}}/\log 2} \quad (2.19)$$

or, comparing the exponents,

$$1 = \frac{kt_{\frac{1}{2}}}{\log 2}, \quad (2.20)$$

which is Eq. 2.3.

2.1.3 Diffusion-limited reactions

Association rates are expected to be less than $\simeq 10^9 \text{ M}^{-1} \text{ s}^{-1}$. All association reactions proceed by the two reactants first finding each other and then reacting. We may estimate the fastest rate at which such association reactions can possibly proceed by assuming that the reactants react immediately once together, so that $t_{\text{reac}} = 0$ in Eq. 2.2. The upper bound on association reactions is then determined from the time taken for the two reactants to diffuse together (t_{diff}). Using the diffusion equation and assuming spherical reactants, this maximum rate is [2] (p. 314)

$$f_{\text{max}} = 4\pi D a \quad (2.21)$$

where D is the sum of the diffusion constants of the reactants and a is the typical size of a reactant.

Remembering that D is measured in units of $\text{m}^2 \text{ s}^{-1}$, f_{max} in Eq. 2.21 has units of volume per second and is the inverse of the time for a pair of reactants to diffuse together in a unit volume. We would like to convert these units to $\text{M}^{-1} \text{ s}^{-1}$ to be able to compare with standard association rates. We therefore multiply first by Avogadro's number so as to consider a mole of reactants diffusing together (similarly to Eq. 2.10) and second by 10^3 to convert the volume units from m^3 to litres:

$$f \text{ (in M)} < f_{\text{max}} \times n_A \times 10^3. \quad (2.22)$$

If D is $1000 \mu\text{m}^2 \text{ s}^{-1}$ and so of order the diffusion constant of water [3] and around 150 times larger than the typical diffusion coefficients of proteins in the cytoplasm [4], and a is 1 nm, then

$$\begin{aligned} f &< 4\pi \times \overbrace{10^3 \times 10^{-12}}^{D \text{ in } \text{m}^2\text{s}^{-1}} \times \overbrace{10^{-9}}^a \times \overbrace{6 \times 10^{23}}^{n_A} \times \overbrace{10^3}^{\text{for } \ell} \\ &\simeq 7.5 \times 10^9 \text{ M}^{-1}\text{s}^{-1}. \end{aligned} \quad (2.23)$$

2.1.4 The concentration of one molecule

A bacterium such as *Escherichia coli* has a volume of approximately $1 \mu\text{m}^3$ or 10^{-18} m^3 or 10^{-15} litres. The concentration of one molecule is then $1/n_A/10^{-15} \text{ M}$ or of order 1 nM. The budding yeast *Saccharomyces cerevisiae* has a volume of approximately $60 \mu\text{m}^3$ or 60×10^{-15} litres. The concentration of one molecule is then of order 10 pM. A human fibroblast has a volume of approximately $10^4 \mu\text{m}^3$ and so the concentration of one molecule is of the order of 0.1 pM.

so that the rate of association of A and B equals the rate of dissociation of C . The equilibrium dissociation constant is defined as $K_{\text{eq}} = b/f$, and

$$[A][B] = K_{\text{eq}}[C]. \quad (2.29)$$

From the rate equations

$$\frac{d[A]}{dt} = \frac{d[B]}{dt} = -f[A][B] + b[C] = -\frac{d[C]}{dt} \quad (2.30)$$

we see that

$$\frac{d[A]}{dt} + \frac{d[C]}{dt} = 0 \quad (2.31)$$

and

$$\frac{d[B]}{dt} + \frac{d[C]}{dt} = 0 \quad (2.32)$$

implying

$$[A] + [C] = A_0 \quad (2.33)$$

and

$$[B] + [C] = B_0 \quad (2.34)$$

for some constant A_0 and B_0 . These conservation laws arise because each C molecule ‘contains’ an A molecule and a B molecule. Together with Eq. 2.29, the conservation laws, Eq. 2.33 and Eq. 2.34, define the equilibrium concentrations of $[A]$, $[B]$, and $[C]$.

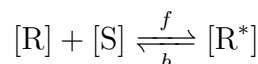
2.3 The law of mass action

The law of mass action states that the rate of a reaction should depend on its stoichiometry in the same way that equilibrium constants depend on the stoichiometry. The stoichiometry of a reaction is defined as the relative numbers of reactants and products that are expended and created by the reaction. For example, for the association reaction $A + B \rightarrow C$, the stoichiometric coefficient of A is -1, of B is -1, and of C is 1 because one molecule of A combines with one molecule of B to form one molecule of C . Comparing Eq. 2.11 and Eq. 2.28, we see that the dependence on stoichiometry is the same because the concentrations are raised to the same powers.

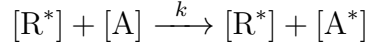
Effectively, the law of mass action means that the rate of a reaction is proportional to the number of ways the reaction can occur, which is the logic we used to derive Eq. 2.11. Using the law of mass action, we ensure that the dynamics of our system are such that the system reaches a thermodynamically correct equilibrium.

2.4 Modelling signal transduction I

To begin our model of a biochemical signalling pathway, consider a receptor, R , in the plasma membrane that enters an activated state R^* when bound by an extracellular signalling molecule, S (Fig. 1). We can model this activation by a binary reaction:



To allow the activated receptors to activate a downstream signalling protein, A say, we include another binary reaction:



Here $[R^*]$ appears on both sides of the chemical equation because R^* is not consumed by the reaction, but catalyses the conversion of A to its activated form A^* .

The corresponding differential equations are

$$\begin{aligned} \frac{d[S]}{dt} &= -f[R][S] + b[R^*] \\ \frac{d[R]}{dt} &= -f[R][S] + b[R^*] \\ \frac{d[R^*]}{dt} &= f[R][S] - b[R^*] \\ \frac{d[A]}{dt} &= -k[A][R^*] \\ \frac{d[A^*]}{dt} &= k[A][R^*] \end{aligned} \tag{2.35}$$

but our main focus of interest is the production of A^* because A^* signals to the interior of the cell that molecules of S are present exterior to the cell.

We will therefore assume that the binding of S to R is at equilibrium so that

$$f[R][S] \simeq b[R^*]. \tag{2.36}$$

The number of receptor molecules is conserved because $d[R]/dt + d[R^*]/dt = 0$: receptors are neither created nor destroyed but only change state from inactivated to activated and vice versa. Writing R_0 for the total concentration of receptors so that

$$R_0 = [R] + [R^*], \tag{2.37}$$

then, using Eq. 2.36, we can show that

$$[R^*] \simeq \frac{[S]R_0}{\frac{b}{f} + [S]}. \tag{2.38}$$

The differential equation for $[A^*]$, the output of the signalling system, then becomes

$$\frac{d[A^*]}{dt} \simeq \frac{k[S]R_0}{\frac{b}{f} + [S]}[A] \tag{2.39}$$

or

$$\frac{d[A^*]}{dt} \simeq \frac{k[S]R_0}{\frac{b}{f} + [S]}(A_0 - [A^*]) \tag{2.40}$$

because the number of A molecules is conserved, with a total concentration of say A_0 , because A also only changes state.

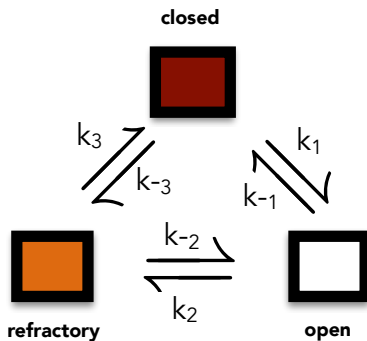
Eq. 2.40 is our model of the signalling pathway. If either $[S] = 0$ or $f = 0$, no A^* is produced. If $[S] \gg b/f$, the rate of production of A^* saturates because all the receptors are bound by S . There is no reverse reaction that converts A^* back into A , and so all the A molecules eventually become activated: $[A^*] \rightarrow A_0$.

2.5 Thermodynamic cycles

A system contains a thermodynamic cycle if it has a series of states interlinked by equilibrium reactions and where starting from any particular state the system can return to that state by passing through a series of intermediate states.

Ion channels often undergo thermodynamic cycles. They can switch from a closed to an open state, which allows ions to pass through the plasma membrane, and then frequently enter a refractory state. In the refractory state, the channel rarely opens but eventually transitions into the closed state, where switching to the open state is more probable.

Schematically these reactions may be written in a circle. The ion channel is said to undergo a thermodynamic cycle because the channel once open can go through the refractory and the closed state before opening again.



If we assume that each of these reactions is at equilibrium and obeys detailed balance then

$$k_1 C = k_{-1} O \quad ; \quad k_2 O = k_{-2} R \quad ; \quad k_3 R = k_{-3} C. \quad (2.41)$$

Rearranging these equations gives

$$C = \frac{k_{-1}}{k_1} O = \frac{k_{-1}}{k_1} \cdot \frac{k_{-2}}{k_2} R = \frac{k_{-1}}{k_1} \cdot \frac{k_{-2}}{k_2} \cdot \frac{k_{-3}}{k_3} C \quad (2.42)$$

and so equilibrium imposes a constraint on the reaction rates:

$$k_1 k_2 k_3 = k_{-1} k_{-2} k_{-3}. \quad (2.43)$$

For a thermodynamic cycle that is able to reach equilibrium, the reaction rates may not be arbitrarily chosen and must obey Eq. 2.43, which implies that the probability of going round the cycle one way is equal to the probability of going round the cycle the other way.

If the rate constants do not satisfy Eq. 2.43, the system is using energy to force the cycle to occur preferentially in one direction. A phenomenon that may not be intended by the modeller.

Aside

We can compute the times to go around the cycle in each direction, which are equal at equilibrium.

Let the typical time for one clockwise transition around the cycle be T_C and so the typical rate for this cycle be $1/T_C$. We expect that the rate of a compound reaction, such as a clockwise transition, is approximately equal to the product of the probability of the most probable reaction and its rate [5]. The most probable clockwise transition is the direct cycle from, say, the closed to the open to the refractory and back to the closed state. Let this probability as $P(c \rightarrow o \rightarrow r \rightarrow c)$ and its rate by $1/t_d$. Then we expect

$$T_C^{-1} \simeq P(c \rightarrow o \rightarrow r \rightarrow c) \times t_d^{-1}. \quad (2.44)$$

Intuitively, the typical clockwise transition time T_+ is longer than the time t_d for a direct clockwise cycle because at least some anticlockwise reactions will also likely occur.

The probability $P(c \rightarrow o \rightarrow r \rightarrow c)$ is a product of the probability of moving from the closed to the open state, $\frac{k_1}{k_{-3}+k_1}$, and the probability of moving from the open to the refractory state, $\frac{k_2}{k_{-1}+k_2}$, and the probability of moving from the refractory back to the closed state, $\frac{k_3}{k_{-2}+k_3}$:

$$P(c \rightarrow o \rightarrow r \rightarrow c) = \frac{k_1}{k_{-3} + k_1} \times \frac{k_2}{k_{-1} + k_2} \times \frac{k_3}{k_{-2} + k_3}. \quad (2.45)$$

The rate of the direct clockwise cycle is the reciprocal of the total dwell time in the three states: closed, open, and refractory. Once the system enters a particular state, the dwell time is the average time spent there. It is determined by the number of reactions leaving the state. The dwell time for the closed state is $\frac{1}{k_{-3}+k_1}$; for the open state it is $\frac{1}{k_{-1}+k_2}$; and for the refractory state $\frac{1}{k_{-2}+k_3}$. The total dwell time is therefore

$$t_d = \frac{1}{k_{-3} + k_1} + \frac{1}{k_{-1} + k_2} + \frac{1}{k_{-2} + k_3}. \quad (2.46)$$

Using Eqs. 2.45 and Eq. 2.46, we can find T_C from Eq. 2.44.

Similarly, if the typical time to transition anticlockwise around the cycle is T_A then we expect

$$T_A^{-1} = P(c \rightarrow r \rightarrow o \rightarrow c) \times t_d^{-1} \quad (2.47)$$

with

$$P(c \rightarrow r \rightarrow o \rightarrow c) = \frac{k_{-3}}{k_{-3} + k_1} \times \frac{k_{-2}}{k_{-2} + k_3} \times \frac{k_{-1}}{k_{-1} + k_2}. \quad (2.48)$$

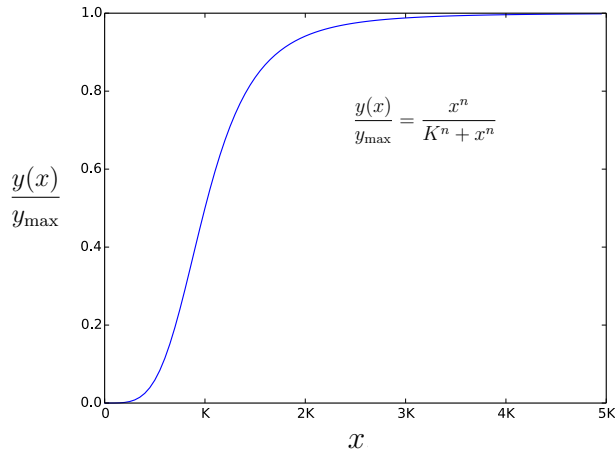
Consequently,

$$\begin{aligned} \frac{T_C}{T_A} &= \frac{P(c \rightarrow r \rightarrow o \rightarrow c)}{P(c \rightarrow o \rightarrow r \rightarrow c)} \\ &= \frac{k_{-1}k_{-2}k_{-3}}{k_1k_2k_3} \end{aligned}$$

which gives Eq. 2.43 when $T_C = T_A$.

2.6 Ultrasensitivity and the Hill number

The response curve of system is its input-output relationship and gives the steady-state level of output as a function of the level of input. Many empirical response curves may be approximately described by a Hill function.



If the output, y , increases with increasing levels of input, x , the appropriate Hill function is

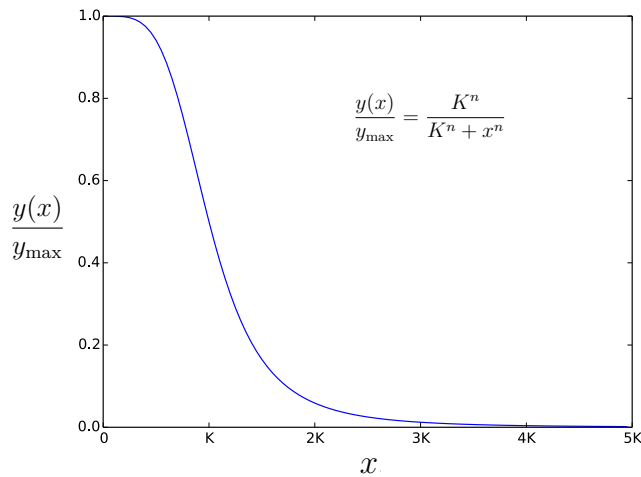
$$\frac{y(x)}{y_{\max}} = \frac{x^n}{K^n + x^n} \quad (2.49)$$

where we call n the Hill number, or occasionally the Hill coefficient, and K is the value of the input that causes the output to be half of its maximum value (y_{\max}). The parameter K is sometimes called the EC_{50} of the response, the half-maximal (50%) effective concentration.

If the output decreases with increasing levels of input, then the appropriate Hill function is

$$\frac{y(x)}{y_{\max}} = \frac{K^n}{K^n + x^n} \quad (2.50)$$

and K is now sometimes called the IC_{50} of the response, the half-maximal inhibitory concentration.



2.7 Describing response curves

The Hill number is often used to characterise the ultrasensitivity of the response. From the definition of the Hill function, its sensitivity at $x = K$ is

$$\left. \frac{d \log y / y_{\max}}{d \log x} \right|_{x=K} = \frac{n}{2} \quad (2.51)$$

and is determined solely by the Hill number. A response with a Hill number of 1 is said to be *hyperbolic*. The rate of a Michaelis-Menten enzymatic reaction as a function of the substrate concentration, Eq. 2.89, is a well-known example. If the Hill number is greater than 1, the response is *ultrasensitive*, and the response curve has a S- or *sigmoidal* shape. With Hill numbers above approximately 3, the response is switch-like or ‘all-or-none’ with little response for inputs below K and an almost maximal response for all inputs above K . This switch-like response is sometimes called a ‘soft’ switch because the underlying system is not bistable (Sec. 4).

For different biochemistry, there is different terminology. Responses with a Hill number greater than 1 are often called ultrasensitive for systems involved in signal transduction and are often called *cooperative* for systems involved in gene regulation. A response with a Hill number below one is *sub-sensitive*.

2.7.1 Sensitivity

With sensitivity analysis, we aim to determine how the behaviour of a model depends on its parameter values. The local sensitivity of a steady-state quantity s with respect to changes in a parameter p is ds/dp . A small change in p , denoted Δp , gives

$$s(p + \Delta p) \simeq s(p) + \frac{ds}{dp} \Delta p + \mathcal{O}(\Delta p^2) \quad (2.52)$$

from a Taylor expansion, or

$$\Delta s = s(p + \Delta p) - s(p) \simeq \frac{ds}{dp} \Delta p. \quad (2.53)$$

The local sensitivity therefore measures how a small Δp affects s . It is, however, unhelpful for comparing different sensitivities because it has units: the units of s divided by the units of p . Different sensitivities may have different units.

The relative local sensitivity is more common; it is dimensionless. We define the relative sensitivity as

$$\chi = \frac{ds/s}{dp/p} = \frac{p}{s} \times \frac{ds}{dp} = \frac{d \log s}{d \log p}. \quad (2.54)$$

From Eq. 2.53,

$$\begin{aligned} \frac{\Delta s}{s} &\simeq \frac{1}{s} \frac{ds}{dp} \times \Delta p \\ &= \frac{p}{s} \frac{ds}{dp} \times \frac{\Delta p}{p} \end{aligned}$$

and so, from Eq. 2.54, the relative sensitivity satisfies

$$\frac{\Delta s}{s} \simeq \chi \frac{\Delta p}{p}. \quad (2.55)$$

The relative sensitivity therefore measures the fractional change in s resulting from a small fractional change in p . Fractional changes are absolute and so make clear what we mean by ‘small’.

The Hill number measures the relative sensitivity of the output y to a change in the input x when the input is at the threshold value, $x = K$. The Hill number, n , is twice the relative sensitivity from Eq. 2.51:

$$n = 2 \left. \frac{d \log y}{d \log x} \right|_{x=K} \quad (2.56)$$

Eq. 2.56 implies that a system with a high sensitivity at the threshold level of input will be a sharp, ultrasensitive switch with a high Hill number. For such systems, a small fractional change in input can cause a large fractional change in output, such as when the input crosses the threshold level.

2.8 Modelling signal transduction II

Considering Fig. 1, we can use a Hill function to immediately write an equivalent to Eq. 2.38:

$$[R^*] \simeq \frac{R_0[S]^n}{K^n + [S]^n} \quad (2.57)$$

where the Hill number n could be greater than 1 if, for example, multiple molecules of S have to bind to a receptor R to activate that receptor or if S only binds to R as a dimer. Eq. 2.40 then becomes:

$$\frac{d[A^*]}{dt} \simeq \frac{kR_0[S]^n}{K^n + [S]^n} (A_0 - [A^*]). \quad (2.58)$$

2.9 Allosterity – and the Monod-Wyman-Changeux model – as a means to generate ultrasensitivity

An enzyme is allosteric if its activity is modified by a regulator binding to a site on the enzyme that is not the enzyme’s functional site. Binding sites on allosteric enzymes interact through conformational changes: a molecule binding at a regulatory site causes a change in conformation at the active site and so alters enzymatic activity.

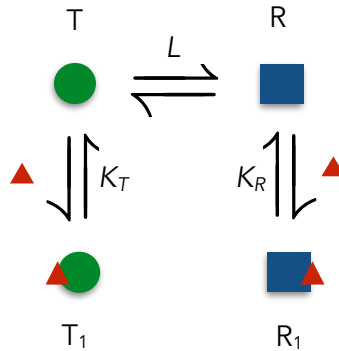
Allosterity explains why a molecule that regulates an enzyme need not have a similar structure to the enzyme’s substrate. This freedom in the structure of regulatory molecules was a great revelation when discovered in the 1950s.

As an example consider a membrane receptor that activates when bound by an extracellular ligand. Biochemically the receptor has two conformational states: one active and one inactive. The active state can signal downstream; the inactive state cannot. An extracellular ligand activates the receptor by preferentially binding to the active state over the inactive one. Through this preference, the ligand stabilises the receptor in the active state. Once active, the receptor may bind a signalling molecule on its cytoplasmic side. This signalling molecule can have a completely different structure from the ligand because the ligand binds to a different site on the receptor.

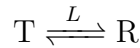
Allosterity is one way to generate ultrasensitive responses, and a celebrated model is the concerted model of Monod, Wyman, and Changeux [6]. In this model, an enzyme has two conformations – arbitrarily called a tense state (denoted T) and a relaxed state (denoted R)

– and spontaneously changes between these conformations. In the tense state, we consider the enzyme to be ‘on’ with high activity; in the relaxed state, it is ‘off’ with low activity. Any molecule that has a higher binding energy for the T state relative to the R state activates the enzyme.

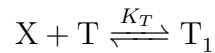
2.9.1 Allosteric molecules with a single binding site for a regulator



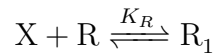
Let a regulatory molecule be X — shown as a red triangle. In the absence of X , we can describe the spontaneous conformational changes as



where L is the equilibrium constant: $L = [R]/[T]$. The binding reactions are second-order:



and



with K_T and K_R being association equilibrium constants – the rate of the association reaction divided by the rate of the dissociation reaction. Let $K_T > K_R$ so that X activates the enzyme because it favours binding the ‘on’ state T .

If there is only one binding site for X on the enzyme and assuming each reaction is at equilibrium:

$$L = \frac{[R]}{[T]} \quad ; \quad [T_1] = K_T[T][X] \quad ; \quad [R_1] = K_R[R][X]. \quad (2.59)$$

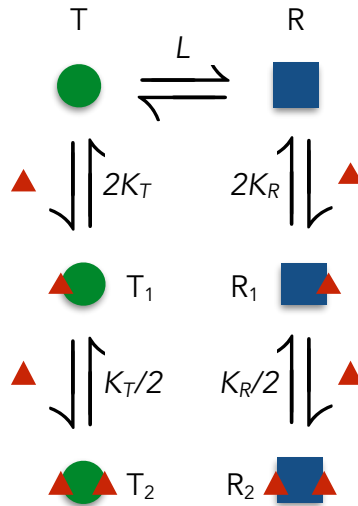
Then the fraction of activated enzymes is

$$\begin{aligned}
 f_{\text{on}} &= \frac{[T] + [T_1]}{[T] + [T_1] + [R] + [R_1]} \\
 &= \frac{[T] + K_T[X][T]}{[T] + K_T[X][T] + L[T] + K_R[X]L[T]} \\
 &= \frac{1 + K_T[X]}{1 + K_T[X] + L(1 + K_R[X])}
 \end{aligned} \quad (2.60)$$

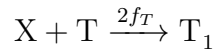
which is a hyperbolic function increasing with $[X]$. The enzymatic activity increases with X because X biases the molecule to adopt the active conformation.

Allowing a two-way reaction between T_1 and R_1 would not change Eq. 2.60. This reaction would not prevent the others from reaching equilibrium, and its equilibrium constant, L_1 say, must obey $L_1 = \frac{K_R}{K_T}L$ because then the set of reactions form a thermodynamic cycle (Sec. 2.5).

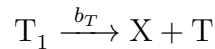
2.9.2 Allosteric molecules with two binding sites for regulators



Allostery can give sharp, switch-like responses as the concentration of the regulatory molecule changes. If the enzyme has two identical binding sites for X and if f_T is the rate of binding one of those sites then the association reaction becomes

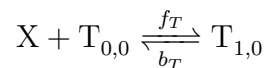


because there are now two choices of binding site for X . Denoting the rate of dissociation by b_T , the dissociation reaction remains

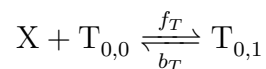


because there is only one way that X can dissociate from T_1 . The overall association constant is therefore $2f_T/b_T = 2K_T$.

We can understand this factor of two by considering explicitly the enzyme's two binding sites for X . Let $T_{0,0}$ denote an enzyme in the tense state with no bound X molecules; $T_{1,0}$ denote a tense enzyme with an X bound to the first site; and $T_{0,1}$ denote a tense enzyme with an X bound to the second site. Then the reactions are



and



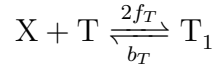
We can write down the differential equation for X , which will have four terms because of the four reactions:

$$\begin{aligned}\frac{d[X]}{dt} &= -f_T[X][T_{0,0}] - f_T[X][T_{0,0}] + b_T[T_{1,0}] + b_T[T_{0,1}] \\ &= -2f_T[X][T_{0,0}] + b_T[T_{1,0}] + b_T[T_{0,1}]\end{aligned}\quad (2.61)$$

If we define $[T_1] = [T_{1,0}] + [T_{0,1}]$ to be the concentration of the enzyme with one molecule of X bound irrespective of where that molecules binds, then Eq. 2.61 becomes

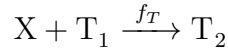
$$\frac{d[X]}{dt} = -2f_T[X][T_{0,0}] + b_T[T_1]\quad (2.62)$$

which is the differential equation that describes the reaction

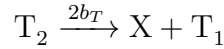


with $T_{0,0}$ written as T . The forward reaction rate increases by a factor of two because there are two possible sites on the enzyme where X can bind and we ignore the particular site where X does bind.

For the binding of a second X , we have



because there is only one binding site for X available on T_1 . The dissociation of an X from T_2 can, however, occur in two ways depending on which X dissociates and whether either $T_{0,1}$ or $T_{1,0}$ forms. So



The overall association constant is consequently $f_T/(2b_T) = K_T/2$. Similar reactions hold for the binding of X to the R -state.

The fraction of activated enzyme can now be a sigmoidal function of the concentration of the regulatory molecule. Assuming equilibrium and so detailed balance for all reactions:

$$L = \frac{[R]}{[T]} \quad ; \quad [T_1] = 2K_T[T][X] \quad ; \quad [T_2] = \frac{K_T}{2}[T_1][X] \quad ; \quad [R_1] = 2K_R[R][X] \quad ; \quad [R_2] = \frac{K_R}{2}[R_1][X]\quad (2.63)$$

Then the fraction of activated enzymes is

$$\begin{aligned}f_{\text{on}} &= \frac{[T] + [T_1] + [T_2]}{[T] + [T_1] + [T_2] + [R] + [R_1] + [R_2]} \\ &= \frac{[T] + 2K_T[X][T] + \frac{1}{2}K_T[X]2K_T[X][T]}{[T] + 2K_T[X][T] + \frac{1}{2}K_T[X]2K_T[X][T] + L[T] + 2K_R[X]L[T] + \frac{1}{2}K_R[X]2K_R[X]L[T]} \\ &= \frac{1 + 2K_T[X] + K_T^2[X]^2}{1 + 2K_T[X] + K_T^2[X]^2 + L(1 + 2K_R[X] + K_R^2[X]^2)} \\ &= \frac{(1 + K_T[X])^2}{(1 + K_T[X])^2 + L(1 + K_R[X])^2}\end{aligned}\quad (2.64)$$

which is a sigmoidal function of $[X]$ with a maximum Hill number of 2.

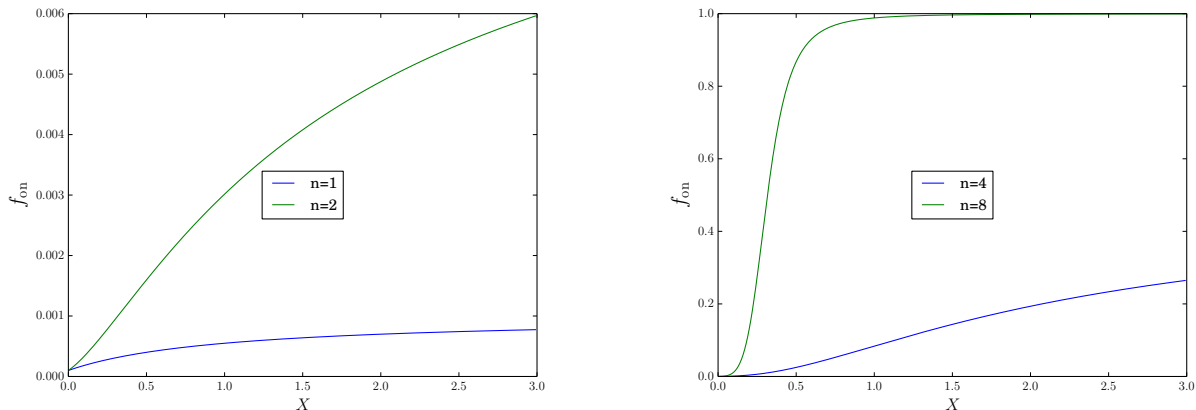


Figure 2: The response curve of an allosteric protein steepens with a higher number of binding sites for ligand. Here $L = 10^4$, $K_T = 10K_R$ and levels of ligand, X , are shown in units of K_R .

2.9.3 Allosteric molecules with n binding sites for regulators

For n binding sites,

$$f_{\text{on}} = \frac{(1 + K_T[X])^n}{(1 + K_T[X])^n + L(1 + K_R[X])^n} \quad (2.65)$$

and the sharpness of the switch increases, with a maximum Hill number of n (Fig. 2). If $[X_{50}]$ is the concentration of X that makes f_{on} half maximal, so that $f_{\text{on}} = \frac{1}{2}$, then Eq. 2.65 implies

$$L(1 + K_R[X_{50}])^n = (1 + K_T[X_{50}])^n. \quad (2.66)$$

Multiplying by $[T]$ and using $[R] = L[T]$, we have that

$$[R](1 + K_R[X_{50}])^n = [T](1 + K_T[X_{50}])^n \quad (2.67)$$

showing that the total concentrations of relaxed and tense allosteric molecules are equal at $[X] = [X_{50}]$, as expected.

Considering the behaviour near $[X] = [X_{50}]$ helps build intuition on why the response becomes more sigmoidal for larger n . By differentiating Eq. 2.65, we can show that the rate at which f_{on} changes with $[X]$ is proportional to n :

$$\left. \frac{\partial f_{\text{on}}}{\partial [X]} \right|_{[X_{50}]} = \frac{n}{4} \cdot \frac{K_T - K_R}{(1 + K_R[X_{50}])(1 + K_T[X_{50}])}. \quad (2.68)$$

This gradient increases with increasing $[X]$ if X binds preferentially to the T states, $K_T > K_R$; the gradient decreases with increasing $[X]$ if X binds preferentially to the R state, $K_T < K_R$. When $[X] = [X_{50}]$, a small increase in the concentration of X will shift the equilibrium for each of X 's binding reactions towards having more X bound. For an allosteric molecule with n binding sites for X , all n reactions will shift, with those involving tense molecules increasing f_{on} by an amount proportional to nK_T , and those involving relaxed molecules decreasing f_{on} by an amount proportional to nK_R , giving the positive and negative terms in Eq. 2.68.

With more than one binding site for the regulatory molecule, the Monod, Wyman, and Changeux model assumes that all the enzyme's binding sites transition together – in a concerted

manner – between the two conformational states [6]. All binding sites on the enzyme are therefore always in the same conformational state. Typically these binding sites are on identical subunits, and we consider each subunit to have the same conformation. Other models of allostery relax the concerted assumption [7].

2.9.4 Limits of the Monod-Wyman-Changeux equation

We can build intuition about Eq. 2.65 by considering various limits.

- Eq. 2.65 always includes basal levels of activation. If there are no input molecules present

$$f_{\text{on}}([X] = 0) = \frac{1}{1 + L} \quad (2.69)$$

and there is basal activation providing $L \ll 1$. Remember that $[T] = [R]/L$, and so $L \ll 1$ implies that molecules are often in the active tense state in the absence of input.

- Full activation is only possible if the input strongly prefers binding to the tense state over the relaxed state. If we add excess input molecules so that both $K_T[X] \gg 1$ and $K_R[X] \gg 1$, then Eq. 2.65 becomes

$$f_{\text{on}}(K_R[X] \gg 1) \simeq \frac{K_T^n}{K_T^n + LK_R^n} \quad (2.70)$$

or, defining the bias in binding to be c so that $K_T = cK_R$,

$$f_{\text{on}} \simeq \frac{c^n}{c^n + L} \quad (2.71)$$

and there is full activation if there is high bias: $c^n \gg L$.

- Eq. 2.65 becomes an activating Hill function for high bias and sufficient input. Writing Eq. 2.65 in terms of K_T and the bias $c = K_T/K_R$

$$f_{\text{on}} = \frac{(1 + K_T[X])^n}{(1 + K_T[X])^n + L(1 + K_T[X]/c)^n} \quad (2.72)$$

then if we have high bias, $c \gg K_T[X]$,

$$f_{\text{on}} \simeq \frac{(1 + K_T[X])^n}{(1 + K_T[X])^n + L}. \quad (2.73)$$

If too we have sufficient input, $K_T[X] \gg 1$, then

$$\begin{aligned} f_{\text{on}} &\simeq \frac{(K_T[X])^n}{(K_T[X])^n + L} \\ &= \frac{[X]^n}{\frac{L}{K_T^n} + [X]^n} \end{aligned} \quad (2.74)$$

which is a Hill equation (Eq. 2.49) with a Hill number equal to n , the number of regulatory binding sites on each allosteric molecule. These limits reduce the system to having essentially two states: $T_n \simeq (K_T X)^n T$ and R , with $[R] = L[T]$.

- Eq. 2.65 becomes an inhibiting Hill function for low bias and sufficient input. Writing Eq. 2.65 in terms of K_R and the bias $c = K_T/K_R$

$$f_{\text{on}} = \frac{(1 + cK_R[X])^n}{(1 + cK_R[X])^n + L(1 + K_R[X])^n} \quad (2.75)$$

then if we have low bias, $c \ll \frac{1}{K_R[X]}$,

$$f_{\text{on}} \simeq \frac{1}{1 + L(1 + K_R[X])^n}. \quad (2.76)$$

If too we have sufficient input, $K_R[X] \gg 1$, then

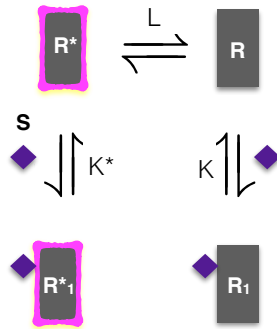
$$\begin{aligned} f_{\text{on}} &\simeq \frac{1}{1 + L(K_R[X])^n} \\ &= \frac{\frac{1}{LK_R^n}}{\frac{1}{LK_R^n} + [X]^n} \end{aligned} \quad (2.77)$$

which is also a Hill function (Eq. 2.50).

Allostery can therefore cause an enzyme to switch sharply between active and inactive states at a threshold concentration of the regulatory molecule. This cooperative behaviour arises because the first regulatory molecule prefers binding to the enzyme's conformational state that favours binding of more regulatory molecules. The bound enzyme will spend more time in this conformation making it easier for a second regulatory molecule to bind. It then becomes even easier for a third molecule to bind.

2.10 Modelling signal transduction III

We can use an allosteric model to describe activation of the receptors in Fig. 1. Consider



then the fraction of activated receptors is

$$f^* = \frac{1 + K^*[S]}{1 + K^*[S] + L(1 + K[S])} \quad (2.78)$$

from Eq. 2.60. The concentration of active receptors is $[R^*] = f^*R_0$, and so Eq. 2.58 becomes

$$\frac{d[A^*]}{dt} \simeq \frac{kR_0(1 + K^*[S])}{1 + K^*[S] + L(1 + K[S])}(A_0 - [A^*]). \quad (2.79)$$

When $[S] = 0$, Eq. 2.79 simplifies

$$\frac{d[A^*]}{dt} \simeq \frac{kR_0}{1 + L}(A_0 - [A^*]) \quad (2.80)$$

and there is a basal rate of activation even in the absence of ligand. This basal rate goes to zero as $L \gg 1$ because then receptors almost never spontaneously enter the activated state.

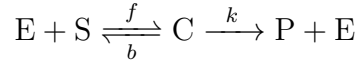
If $K^*[S] \gg 1$ so that almost all the active receptors are in the R_1^* state and not in the R^* state, then Eq. 2.79 becomes

$$\frac{d[A^*]}{dt} \simeq \frac{kR_0K^*[S]}{L + (K^* + KL)[S]}(A_0 - [A^*]) \quad (2.81)$$

and we recover Eq. 2.40.

2.11 Enzyme kinetics

Almost all studies of enzymes start with the framework introduced by Michaelis and Menten, which although approximate is both simple and practical. An enzymatic reaction occurs in two steps: first, the enzyme binds the substrate to form an enzyme-substrate complex; second, catalysis occurs and this complex dissociates to form the product and release the enzyme:



For example, E may be a kinase in a signalling network that phosphorylates a substrate S to form a product P of phosphorylated S .

Using the law of mass action, the rate equations for this system are

$$\begin{aligned} \frac{d[E]}{dt} &= -f[E][S] + (b + k)[C] \\ \frac{d[S]}{dt} &= -f[E][S] + b[C] \\ \frac{d[C]}{dt} &= f[E][S] - (b + k)[C] \\ \frac{d[P]}{dt} &= k[C]. \end{aligned} \quad (2.82)$$

Catalysis does not consume the enzyme, and we see that

$$\frac{d[E]}{dt} + \frac{d[C]}{dt} = 0 \quad (2.83)$$

so that

$$[E] + [C] = [E]_0 + [C]_0 = E_{\text{tot}} \quad (2.84)$$

where the right-hand side is the total amount of enzyme initially present — E_{tot} . Similarly, the substrate is only converted into product and no new substrate is created, so that $[S] + [C] + [P]$ is a constant: the total amount of substrate is conserved in its various forms — either as free substrate, in complex with enzyme, or as product.

The Michaelis-Menten approximation typically relies on more substrate being present than enzyme, often true initially, so that almost all the enzyme is bound in a complex with the substrate. The concentration of the complex then does not change with time, although $[S]$ and $[P]$ do. The concentration of complex remains approximately constant while levels of S remain sufficiently high. We say that $[C]$ is at quasi-steady state because $d[C]/dt \simeq 0$, but the system as a whole is not at steady state, with $d[S]/dt < 0$ and $d[P]/dt > 0$.

If $d[C]/dt \simeq 0$, then

$$f[E][S] = (b + k)[C] \quad (2.85)$$

from Eqs 2.82. Combining Eq. 2.85 with Eq. 2.84, we can show that

$$[C] \simeq \frac{E_{\text{tot}}[S]}{\frac{b+k}{f} + [S]} \quad (2.86)$$

and so

$$\frac{d[P]}{dt} \simeq \frac{kE_{\text{tot}}[S]}{\frac{b+k}{f} + [S]} \quad (2.87)$$

which depends only on the total amount of enzyme and the concentration of the substrate.

Defining

$$V_{\text{max}} = kE_{\text{tot}} \quad ; \quad K_m = \frac{b+k}{f} \quad (2.88)$$

we have the Michaelis-Menten equation:

$$\frac{d[P]}{dt} \simeq \frac{V_{\text{max}}[S]}{K_m + [S]} \quad (2.89)$$

for the initial rate of an enzymatic reaction. The maximum rate of the reaction is given by V_{max} and occurs for high concentrations of substrate. The concentration of substrate at which the reaction occurs at half this rate is given by the Michaelis-Menten constant, K_m .

We have too that

$$\frac{d[S]}{dt} + \frac{d[C]}{dt} + \frac{d[P]}{dt} = 0 \quad (2.90)$$

because the substrate is either free or in a complex with the enzyme or has been converted into the product. The quasi-steady-state assumption, $d[C]/dt \simeq 0$, implies that Eq. 2.90 becomes

$$\frac{d[S]}{dt} \simeq -\frac{d[P]}{dt} \quad (2.91)$$

or

$$\frac{d[S]}{dt} \simeq -\frac{V_{\text{max}}[S]}{K_m + [S]} \quad (2.92)$$

from Eq. 2.89, another form of the Michaelis-Menten equation.

The Michaelis-Menten equation is approximate, and more careful analysis shows that

$$\frac{E_{\text{tot}}}{[S]_0 + K_m} \ll 1 \quad (2.93)$$

is necessary for Eq. 2.89 to hold [8], where $[S]_0$ is the initial concentration of substrate. Eq. 2.93 implies first that the time taken for the enzyme to bind substrate to build the complex C is faster than the time taken for the levels of substrate to change, and, second, that a negligible amount of substrate is lost while the complex forms [8]. The initial condition that we can use with the quasi-steady state approximation is then still $[S(t = 0)] = [S]_0$, the true initial condition of the system.

In the cell, however, enzymes, such as those in metabolism, often operate in the presence of their product, which competes with the substrate to bind to the enzyme and is inhibiting. The Michaelis-Menten equation then no longer holds. Furthermore, metabolic enzymes usually have more than one substrate [9].

2.12 Modelling signal transduction IV

Given our allosteric model of the activation of the receptors in Fig. 1 (Eq. 2.79), we can consider how the signal propagates within the cell and model the dynamics of kinase B , which is activated by A^* . We will assume that this activation obeys Michaelis-Menten kinetics:

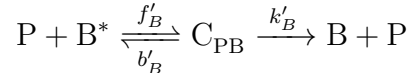


The rate of change of $[B^*]$ then has a positive term

$$\frac{k_B[A^*][B]}{\frac{b_B+k_B}{f_B} + [B]} \quad (2.94)$$

from Eq. 2.87. Note that it is only active A that catalyses the activation of B , and so $[A^*]$ is equivalent to E_{tot} in Eq. 2.87.

If there is an enzyme that is constitutively active and de-activates B^* , such as a phosphatase if A^* is a kinase, then this enzyme too is likely to have Michaelis-Menten kinetics. Denoting the enzyme as P , we have



and so a negative term in the rate of change of $[B^*]$ of

$$-\frac{k'_B[P][B^*]}{\frac{b'_B+k'_B}{f'_B} + [B^*]} \quad (2.95)$$

Hence

$$\frac{d[B^*]}{dt} \simeq \frac{k_B[A^*][B]}{\frac{b_B+k_B}{f_B} + [B]} - \frac{k'_B[P][B^*]}{\frac{b'_B+k'_B}{f'_B} + [B^*]} \quad (2.96)$$

or

$$\frac{d[B^*]}{dt} \simeq \frac{k_B[A^*](B_0 - [B^*])}{\frac{b_B+k_B}{f_B} + B_0 - [B^*]} - \frac{k'_B[P][B^*]}{\frac{b'_B+k'_B}{f'_B} + [B^*]} \quad (2.97)$$

because the total concentration of B is conserved and here equal to $B_0 = [B] + [B^*]$. Often the assumption that enzyme P works far from saturation is made so that $[B^*] \ll \frac{b'_B+k'_B}{f'_B}$. Eq. 2.97 then simplifies

$$\frac{d[B^*]}{dt} \simeq \frac{k_B[A^*](B_0 - [B^*])}{\frac{b_B+k_B}{f_B} + B_0 - [B^*]} - d_B[B^*] \quad (2.98)$$

where

$$d_B = \frac{f'_B k'_B [P]}{b'_B + k'_B}. \quad (2.99)$$

Including similar activation of molecule C by B^* , our final model of the cytoplasmic reactions of Fig. 1 is

$$\begin{aligned} \frac{d[A^*]}{dt} &= \frac{k_A R_0 (1 + K^*[S])}{1 + K^*[S] + L(1 + K[S])} (A_0 - [A^*]) - d_A [A^*] \\ \frac{d[B^*]}{dt} &= \frac{k_B [A^*] (B_0 - [B^*])}{\frac{b_B + k_B}{f_B} + B_0 - [B^*]} - d_B [B^*] \\ \frac{d[C^*]}{dt} &= \frac{k_C [B^*] (C_0 - [C^*])}{\frac{b_C + k_C}{f_C} + C_0 - [C^*]} - d_C [C^*] \end{aligned} \quad (2.100)$$

assuming that deactivating enzymes, the phosphatase, are present and far from saturation.

2.13 Enzymatic cascades

Enzymatic cascades, where the first enzyme in the cascade activates the second and the second in turn activates the third and so on, have the potential to generate response curves that are ultrasensitive. A well understood example involves the MAP kinases involved in the maturation of oocytes in the frog *Xenopus laevis*. The hormone progesterone activates the MAP kinase kinase kinase Mos; Mos activates the MAP kinase kinase MEK1; and MEK1 activates the MAP kinase p42. Activation of p42 MAP kinase leads ultimately to the oocyte maturing.

If each step of the cascade is ultrasensitive, then each subsequent step increases the ultrasensitivity of the response of the cascade's final enzyme. For example, if steady-state $[B^*]$ is a sigmoidal function of $[A^*]$ then

$$[B^*] = [B^*]_{\max} \cdot \frac{[A^*]^{n_B}}{K_B^{n_B} + [A^*]^{n_B}} \quad (2.101)$$

where n_B is the Hill number and K_B is the EC_{50} of the activation of B by A^* . Similarly, if steady-state $[C^*]$ is a sigmoidal function of $[B^*]$ then

$$[C^*] = [C^*]_{\max} \cdot \frac{[B^*]^{n_C}}{K_C^{n_C} + [B^*]^{n_C}} \quad (2.102)$$

where n_C is the Hill number and K_C is the EC_{50} of B^* . Inserting Eq. 2.101 into Eq. 2.102 gives

$$[C^*] = [C^*]_{\max} \cdot \frac{\left([B^*]_{\max} \frac{[A^*]^{n_B}}{K_B^{n_B} + [A^*]^{n_B}} \right)^{n_C}}{K_C^{n_C} + \left([B^*]_{\max} \frac{[A^*]^{n_B}}{K_B^{n_B} + [A^*]^{n_B}} \right)^{n_C}}. \quad (2.103)$$

If the concentration of A^* is smaller than its EC_{50} , meaning that $[A^*] \ll K_B$, then

$$[C^*] \simeq [C^*]_{\max} \cdot \frac{[A^*]^{n_B n_C}}{\frac{K_B^{n_B n_C} K_C^{n_C}}{[B^*]_{\max}^{n_C}} + [A^*]^{n_B n_C}} \quad (2.104)$$

and the maximum effective Hill number of the response of C^* to A^* is $n_B n_C$ — the product of the Hill numbers of each stage of the cascade.

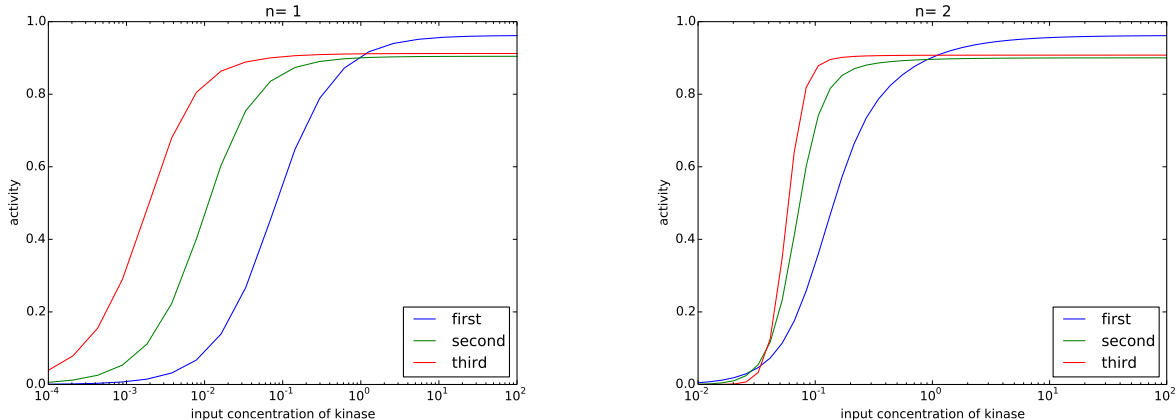


Figure 3: Enzymes lower in a cascade respond more sigmoidally than enzymes higher in the cascade if the Hill number for activation of each step, n , is greater than 1.

For example, if each element of the cascade has a Hill number of two then a cascade of three enzymes would have a maximum Hill number of $2^3 = 8$. In contrast, if each element of the cascade responds hyperbolically ($n = 1$) then the cascade will have a maximum Hill number of one regardless of the number of stages in the cascade (Fig. 3).

How could each element of the cascade have a Hill number greater than one? If a kinase needs to be phosphorylated only once by an upstream kinase to become active then it is difficult to generate ultrasensitivity without having to impose restrictions on the concentrations of the enzymes [10]. Many kinases, including many MAP kinases, require, however, two phosphorylations to become active. If the activating kinase acts distributively and dissociates from the downstream kinase after each phosphorylation, then activation of the downstream kinase ‘sees’ the concentration of the upstream kinase twice, once for each phosphorylation. For a processive kinase, which binds and phosphorylates the substrate twice before dissociating, the concentration of the upstream kinase is seen only once. We therefore might expect activation of a kinase by a distributive upstream kinase to be a sigmoidal function of that upstream kinase’s concentration. Where tested, this expectation has been borne out [11].

2.14 Zero-order ultrasensitivity

A kinase and a phosphatase acting on the same substrate can generate a highly ultrasensitive response in the level of phosphorylated substrate as the ratio of the concentration of the two enzymes is varied [10]. A substrate that is continually phosphorylated and then dephosphorylated is sometimes said to take part in a ‘futile’ cycle because energy appears to be pointlessly consumed. Such cycles may, however, be used by the cell to generate ultrasensitive responses.

For example, consider a kinase and a phosphatase that bind identically to a substrate and either phosphorylate or dephosphorylate with the same rate. If there are initially equal amounts of both enzymes then half of the substrate is phosphorylated at steady state. Let both enzymes be saturated – there is so much substrate compared to enzymes that both the kinase and the phosphatase work close to their maximum rate and no longer have a Michaelis-Menten dependence on the concentration of their substrate. If there is a small increase in the concentration

of one of the enzymes, say the phosphatase, then the kinase is unable to resist the increase in phosphatase activity because the kinase is already working at its maximum rate. The extra phosphatases act as if they are unopposed, and there is a sharp switch in the phosphorylated state of the substrate with the substrate becoming mostly unphosphorylated. Similarly, a small increase in the concentration of the kinase away from the symmetric case leads to a switch to mostly phosphorylated substrate.

This ultrasensitive switch is referred to as ‘zero-order’ because both enzymes should be saturated and work at a constant, or zero-order, rate. If the enzymes are not saturated, then a small increase in the concentration of, say, the kinase can be opposed by the phosphatase: the activity of the phosphatase also increases because of the increase in concentration of phosphorylated substrate, following the Michaelis-Menten equation (Eq. 2.89). Zero-order ultrasensitive responses can switch sharply and can have Hill numbers greater than 10.

2.15 Summary

Models of biochemical systems are typically formulated using the law of mass action and so each chemical reaction proceeds at a rate proportional to the number of ways that the reaction can occur.

Without input of energy, all systems tend to equilibrium. Equilibrium is a special case of a steady state, where each individual reaction is balanced by an opposing reaction. This condition of detailed balance means that no work can be extracted from the equilibrium state, and so all living cells can be at steady state but not at equilibrium. Equilibrium in a thermodynamic cycle imposes a condition on the rates of the reactions, and they cannot all be freely chosen.

Several simplifying approximations that do not obey the law of mass action are often used for rates of reactions, but we can derive these approximations from system with dynamics that do obey the law of mass action. The Hill function describes a generic reaction rate that involves switch-like behaviour and does not satisfy mass action. The Michaelis-Menten rate of an enzymatic reaction has a Hill number of one, and the Monod-Wyman-Changeux model of allostery has a maximum Hill number determined by the number of subunits in the allosteric molecule. Ultrasensitive responses can have Hill numbers that give perfect switching (either all molecules ‘off’ or all molecules ‘on’). Under certain conditions, cascades of switches have a Hill number that is the product of the Hill numbers for each individual stage.

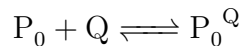
3 Modelling gene expression

Gene expression is fundamental to much of biology and modelling gene expression is fundamental to much of systems biology. We can use equations of chemical reactions to describe binding of proteins to promoters and to describe transcription and translation. To understand the average behaviour of a system, we typically model how occupied the promoters of interest are by transcription factors and RNA polymerase on average.

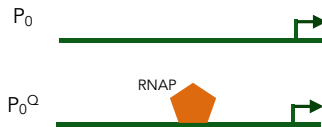
To proceed, we assume that binding of proteins to the DNA occurs faster than transcription, translation, and the degradation of both mRNAs and proteins so that each binding reaction is at equilibrium. We will derive expressions for the promoter occupancy by assuming that the DNA-binding reactions are at equilibrium, but identical expressions can be found too using ideas from statistical mechanics [12].

3.1 Modelling constitutive expression

A constitutively expressed gene is unregulated and synthesises mRNA at a constant average rate. The promoter therefore has two states: it can be either unbound or bound by RNA polymerase. If Q denotes RNA polymerase and P_0 is the unoccupied promoter then



describes the binding of RNA polymerase to the promoter. P_0^Q is the complex of the promoter bound by RNA polymerase:



At equilibrium,

$$P_0^Q = K_Q Q P_0 \tag{3.1}$$

where Q here represents the number of molecules of Q , which we can convert into a concentration $[Q]$ by dividing both sides of the equation by the volume of the cell. K_Q is an association constant. We expect $K_Q > 1$ because it is determined by polymerases's binding energy to the DNA, ΔG_b , via $K_Q = e^{-\frac{\Delta G_b}{RT}}$ [12], and $\Delta G_b < 0$.

The number of molecules of the promoter do not change with these reactions — the promoter only changes state — and, assuming n copies of the promoter, we can write down a conservation law:

$$P_0 + P_0^Q = n. \tag{3.2}$$

Using Eq. 3.1, this conservation implies that

$$P_0 + K_Q Q P_0 = n \tag{3.3}$$

and so that

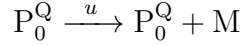
$$P_0 = \frac{n}{1 + K_Q Q} \tag{3.4}$$

which is the average number of promoters that are free and not bound by RNA polymerase. From Eq. 3.1, the average number of bound promoters is

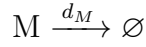
$$P_0^Q = \frac{nK_Q Q}{1 + K_Q Q}. \quad (3.5)$$

3.1.1 Modelling transcription

Transcription occurs only when RNA polymerase Q is bound



where u is the rate at which RNA polymerase initiates transcription. We assume that the binding of RNAP at the promoter is fast compared to u and remains at equilibrium so that a bound polymerase replaces the one that leaves the DNA after it finishes transcribing. If the mRNA is degraded



then the rate equation for the mRNA M is

$$\frac{dM}{dt} = uP_0^Q - d_M M \quad (3.6)$$

and the half-life of mRNA is $\log(2)/d_M$ (see Sec. 2.1.2).

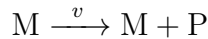
Eq. 3.1 and Eq. 3.4 imply that Eq. 3.6 can be written as

$$\frac{dM}{dt} = \frac{nuK_Q Q}{1 + K_Q Q} - d_M M. \quad (3.7)$$

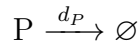
We can see that the rate of transcription increases as the number of RNA polymerase molecules increase and saturates at a maximum rate of nu .

3.1.2 Modelling translation

Translation is usually modelled as a first-order process with rate, say, v :



for mRNA, M , and protein, P . With first-order degradation of proteins,



the equation for protein dynamics is then

$$\frac{dP}{dt} = vM - d_P P \quad (3.8)$$

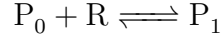
with d_P being the protein degradation rate. The half-life of protein is $\log(2)/d_P$. In Eq. 3.8, M is a function of time and obeys Eq. 3.7.

Eq. 3.7 and Eq. 3.8 together model constitutive gene expression.

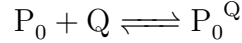
3.2 Repression by a single repressor

The average rate of transcription is a Hill function of the concentration of repressor with a Hill number of one if the repressor binds to a single site on the DNA.

Let P_0 denote the free promoter of a gene of interest and let P_1 denote the promoter when a repressor is bound. Then



for repressor, R . The binding of the repressor prevents RNA polymerase from binding to the promoter and so stops transcription. In the absence of repressor, RNA polymerase, denoted Q , can bind to the promoter

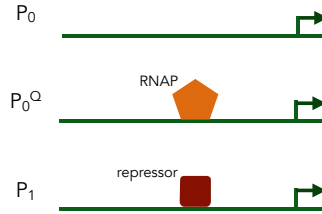


and initiate transcription with a rate u .

If both these binding reactions are at equilibrium then

$$P_1 = K_R R P_0 \quad ; \quad P_0^Q = K_Q Q P_0 \quad (3.9)$$

where K_R and K_Q are association constants and increase in magnitude if binding to the promoter becomes stronger.



The number of molecules of the promoter do not change with these reactions and, assuming n molecules in total, we can write:

$$P_0 + P_0^Q + P_1 = n \quad (3.10)$$

Using Eq. 3.9, this conservation implies that

$$P_0 + K_Q Q P_0 + K_R R P_0 = n \quad (3.11)$$

and so that

$$P_0 = \frac{n}{1 + K_Q Q + K_R R} \quad (3.12)$$

which is the average number of promoters that are free and bound by neither the repressor nor RNA polymerase. From Eq. 3.9, the average number of promoters that are able to transcribe – have a bound RNA polymerase – is

$$P_0^Q = \frac{n K_Q Q}{1 + K_Q Q + K_R R} \quad (3.13)$$

The rate equation describing transcription is then

$$\frac{dM}{dt} = u P_0^Q - d_M M \quad (3.14)$$

or, from Eq. 3.13,

$$\frac{dM}{dt} = \frac{nuK_QQ}{1 + K_QQ + K_RR} - d_M M. \quad (3.15)$$

We may write Eq. 3.15 as

$$\frac{dM}{dt} = \frac{\left(\frac{nuK_QQ}{1+K_QQ}\right)}{1 + \left(\frac{K_R}{1+K_QQ}\right) R} - d_M M \quad (3.16)$$

which has the form of a Hill function in the concentration of repressor if the number of free RNA polymerases is approximately constant.

We can further write

$$\frac{dM}{dt} = u_{\max} \left[\frac{1}{1 + \frac{R}{K_1}} \right] - d_M M \quad (3.17)$$

where the maximum rate of transcription is $u_{\max} = \frac{nuK_QQ}{1+K_QQ}$ and the half-maximal number of repressors is $K_1 = \frac{1+K_QQ}{K_R}$. Note that both these quantities are functions of the numbers of free RNA polymerase, Q .

We again model translation as a first-order process:

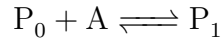
$$\frac{dP}{dt} = vM - d_P P \quad (3.18)$$

where M satisfies Eq. 3.17.

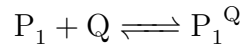
3.3 Activation by a single activator

The average rate of transcription can also be a Hill function with a Hill number of one if transcription is controlled by the binding of a single activator.

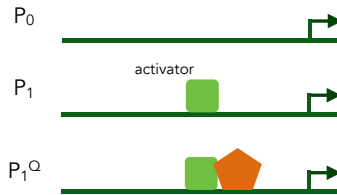
We will proceed as before and consider the binding of activator, A , to the free promoter



as well as the binding of RNA polymerase to the promoter when activator is already bound



We will assume further that transcription only occurs from this P_1^Q state.



When the number of promoters is conserved and all reactions involving DNA binding are at equilibrium

$$P_1 = K_A A P_0 \quad ; \quad P_1^Q = K'_Q Q P_1, \quad (3.19)$$

where K_A and K'_Q are association constants, and

$$P_0 + P_1 + P_1^Q = n \quad (3.20)$$

where n is the number of promoters.

Combining Eq. 3.19 and Eq. 3.20 implies that

$$P_1^Q = \frac{nK'_Q K_A A Q}{1 + K_A A + K'_Q K_A A Q} \quad (3.21)$$

for the average number of promoters occupied by RNA polymerase. If u is the rate of transcription when both polymerase and activator are bound then mRNAs obey

$$\frac{dM}{dt} = \frac{uK'_Q Q K_A A}{1 + K_A A + K'_Q K_A A Q} n - d_M M \quad (3.22)$$

with first-order degradation. We can re-write the average rate of transcription as a function of only two parameters if Q is constant:

$$\begin{aligned} \frac{dM}{dt} &= \frac{(nuK'_Q Q)K_A A}{1 + (1 + K'_Q Q)K_A A} - d_M M \\ &= \frac{\left(\frac{nuK'_Q}{1+K'_Q Q}\right)(1 + K'_Q Q)K_A A}{1 + (1 + K'_Q Q)K_A A} - d_M M \\ &= u_{\max} \left[\frac{\frac{A}{K_1}}{1 + \frac{A}{K_1}} \right] - d_M M \end{aligned} \quad (3.23)$$

with $u_{\max} = \frac{nuK'_Q Q}{1+K'_Q Q}$ and $K_1^{-1} = (1 + K'_Q Q)K_A$, and the average transcriptional rate is a Hill function with a Hill number of one.

3.4 Activation by two activators

We can extend this approach to promoters that bind multiple transcription factors. For example, consider a promoter that has binding sites for two activators and can initiate transcription only when activators bind both sites. Denoting P_{00} as the free promoter, P_{10} and P_{01} as the promoter when a transcription factor binds one site, and P_{11} as the promoter when transcription factors bind both sites, then we have



and

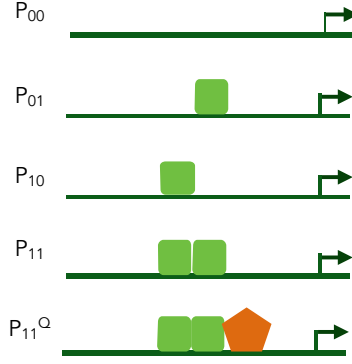


If these reactions are at equilibrium, we can write

$$P_{10} = K_{10} A P_{00} \quad ; \quad P_{01} = K_{01} A P_{00} \quad (3.24)$$

and

$$P_{11} = \tilde{K}_{10} A P_{01} \quad ; \quad P_{11} = \tilde{K}_{01} A P_{10} \quad (3.25)$$

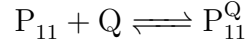


with K_{10} , K_{01} , \tilde{K}_{10} , and \tilde{K}_{01} being association constants and the tilde denoting binding when another activator is already bound.

Eq. 3.24 and Eq. 3.25 form a thermodynamic cycle and so a relationship exists between the equilibrium association constants

$$K_{01}\tilde{K}_{10} = K_{10}\tilde{K}_{01} \quad (3.26)$$

because at equilibrium there should be nothing unique about the route taken to form P_{11} , whether the activator binds initially to either the first or the second binding site. Finally, let us assume that RNA polymerase can only bind to the promoter when activators bind both their sites



and so

$$P_{11}^Q = K'_Q Q P_{11} \quad (3.27)$$

at equilibrium, with Q being the number of free polymerases.

Again we have a fixed number of promoters

$$P_{00} + P_{10} + P_{01} + P_{11} + P_{11}^Q = n \quad (3.28)$$

which implies that

$$P_{00} + K_{10}AP_{00} + K_{01}AP_{00} + \tilde{K}_{10}K_{01}A^2P_{00} + \tilde{K}_{10}K_{01}K'_QQA^2P_{00} = n \quad (3.29)$$

and so

$$P_{11}^Q = \frac{nK'_Q\tilde{K}_{10}K_{01}QA^2}{1 + K_{10}A + K_{01}A + \tilde{K}_{10}K_{01}A^2 + \tilde{K}_{10}K_{01}K'_QQA^2} \quad (3.30)$$

is the average number of promoters occupied by RNA polymerase.

Letting

$$\tilde{K}_{10} = K_i K_{10} \quad (3.31)$$

with K_i greater than one and determined by the free energy of interaction between both activators when bound at the promoter, $K_i = e^{-\frac{\Delta G_{\text{int}}}{RT}}$, then the number of mRNAs obeys

$$\frac{dM}{dt} = \frac{unK'_QQK_iK_{10}K_{01}A^2}{1 + K_{10}A + K_{01}A + K_iK_{10}K_{01}A^2 + K_iK_{10}K_{01}K'_QQA^2} - d_M M \quad (3.32)$$

with u being the rate of transcription from promoter state P_{11}^Q . The average rate of transcription depends on three parameters if the number of free RNA polymerases is approximately constant

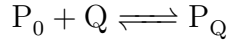
$$\frac{dM}{dt} = u_{\max} \left[\frac{\frac{A^2}{K_2^2}}{1 + \frac{A}{K_1} + \frac{A^2}{K_2^2}} \right] - d_M M \quad (3.33)$$

with $u_{\max} = \frac{unK'_Q Q}{1+K'_Q Q}$, $K_1^{-1} = K_{01} + K_{10}$, and $K_2^{-2} = K_i K_{10} K_{01} (1 + K'_Q Q)$. The maximal Hill number is two.

Note that if $\tilde{K}_{10} = K_i K_{10}$ then $\tilde{K}_{01} = K_i K_{01}$ because the energy of interaction between the activators is the same in both cases. Note too that Eq. 3.26 is then satisfied, as expected.

3.4.1 Multiple transcriptionally active states

We can extend this model by allowing RNAP to bind to the promoter in the absence of the activators too:



with $P_Q = K_Q Q P_0$. If u_ℓ is the rate of transcription from this state — such unregulated transcription is sometimes called leakage, then Eq. 3.32 becomes

$$\frac{dM}{dt} = n \frac{u_\ell K_Q Q + u K'_Q Q K_i K_{10} K_{01} A^2}{1 + K_Q Q + K_{10} A + K_{01} A + K_i K_{10} K_{01} A^2 + K_i K_{10} K_{01} K'_Q Q A^2} - d_M M \quad (3.34)$$

with a new $K_Q Q$ term appearing in the numerator and the denominator because we are considering an extra state of the promoter that is transcriptionally active — the P_Q state. If Q is constant, we can simplify to write

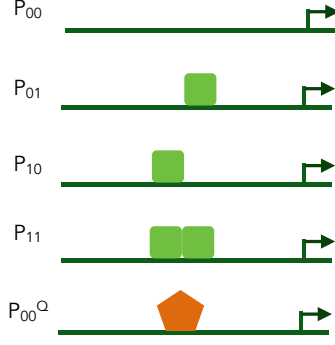
$$\frac{dM}{dt} = \frac{u_{\text{basal}} + u_{\max} \times \frac{A^2}{K_2^2}}{1 + \frac{A}{K_1} + \frac{A^2}{K_2^2}} - d_M M \quad (3.35)$$

but now with $K_1^{-1} = \frac{K_{01} + K_{10}}{1 + K_Q Q}$ and $K_2^{-2} = K_i K_{10} K_{01} \frac{1 + K'_Q Q}{1 + K_Q Q}$ and with a basal rate of transcription of $u_{\text{basal}} = \frac{u_\ell n K_Q Q}{1 + K_Q Q}$. As before, $u_{\max} = \frac{unK'_Q Q}{1 + K'_Q Q}$. For the activators to be efficient, RNAP should prefer to bind to the promoter when two activators have already bound, $K'_Q > K_Q$, and the rate of transcription should be highest from this state, so that $u > u_\ell$.

3.5 General regulation

There is a pattern in the expressions for the average rate of transcription, one expected from statistical mechanics [12]. Each term in the denominator represents a possible state of the promoter: we represent the free state by the number 1 and a bound state by the product of the association constants for each binding event times the number of ways those binding events can occur. Each term in the numerator represents a state of the promoter from which transcription can occur. We multiply each of these terms by their rate of transcription and by the number of promoters.

For example, consider a promoter with two binding sites for repressors where the binding of a repressor to either site prevents the binding of RNA polymerase. The promoter then has



five states: free, bound by polymerase, one site bound by a repressor, the other site bound by a repressor, and both sites bound by a repressor. The denominator of the average rate of transcription is

$$1 + K_Q Q + K_{01} R + K_{10} R + K_{11} R^2 \quad (3.36)$$

and the numerator is

$$nu \times K_Q Q. \quad (3.37)$$

Three factors determine the association constant K_{11} for two repressors binding simultaneously to the promoter: the change in free energy of one repressor binding, which determines its association constant; the change in free energy of another binding, or its association constant; and the free energy of interaction between two bound repressors. As before, we have $K_{11} = K_{01} K_{10} K_i$. Therefore the number of mRNAs satisfies the rate equation:

$$\frac{dM}{dt} = nu \frac{K_Q Q}{1 + K_Q Q + K_{01} R + K_{10} R + K_i K_{10} K_{01} R^2} - d_M M \quad (3.38)$$

which we can write as

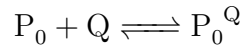
$$\frac{dM}{dt} = \frac{nu K_Q Q}{1 + K_Q Q} \left[\frac{1}{1 + \frac{K_{01} + K_{10}}{1 + K_Q Q} R + \frac{K_i K_{10} K_{01}}{1 + K_Q Q} R^2} \right] - d_M M. \quad (3.39)$$

The maximal Hill number is two.

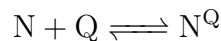
3.6 Including non-specific binding to DNA

Although transcriptional regulators have a preferred DNA sequence, one that they bind to strongly, there will be similar sequences in the genome where the regulator may bind weakly. We can include the effect of this non-specific binding in our models of transcriptional regulation [12].

Let's begin with RNA polymerase. As before, we have specific binding to the promoter of interest, P_0 ,



but now we include non-specific binding to other sites on the DNA, which we will call N :



We expect the number of non-specific binding sites, n_Q say, to be much larger than the number of specific ones: $n_Q \gg n$.

With both binding reactions at equilibrium

$$P_0^Q = K_Q Q P_0 \quad ; \quad N^Q = K_Q^N N Q \quad (3.40)$$

for association constants K_Q and K_Q^N . Writing m_Q for the number of RNA polymerase molecules available to transcribe our gene of interest and providing this number does not change over the time we wish to model, we have that

$$Q + P_0^Q + N^Q = m_Q \quad (3.41)$$

or

$$Q + K_Q Q P_0 + K_Q^N N Q = m_Q. \quad (3.42)$$

The number of free polymerases, Q , satisfies

$$Q = \frac{m_Q}{1 + K_Q P_0 + K_Q^N N}. \quad (3.43)$$

The number of polymerases binding non-specifically should be much greater than the number binding specifically: $N^Q \gg P_0^Q$, or $K_Q^N N \gg K_Q P_0$ from Eq. 3.40, because there are so many more non-specific binding sites. Therefore

$$Q \simeq \frac{m_Q}{1 + K_Q^N N} \quad (3.44)$$

from Eq. 3.43.

We can simplify further. The number of non-specific binding sites satisfies

$$N + N_Q = n_Q \quad (3.45)$$

or

$$\begin{aligned} N &= \frac{n_Q}{1 + \frac{N_Q}{N}} \\ &\simeq n_Q \end{aligned} \quad (3.46)$$

because we expect most non-specific sites to be free, $N_Q \ll N$. Eq. 3.44 becomes

$$Q \simeq \frac{m_Q}{1 + K_Q^N n_Q}. \quad (3.47)$$

From Eq. 3.47, non-specific binding reduces the number of Q molecules available to bind specifically to the promoter. The more non-specific binding sites, the greater n_Q , and the stronger the association constant for binding to these sites, the greater K_Q^N , the fewer polymerases are available to bind specifically. If there is no non-specific binding, $n_Q = 0$, and $Q \simeq m_Q$.

Although we focused on RNA polymerase, the same argument holds for any transcriptional regulator, and so the number of free repressor molecules is

$$R \simeq \frac{m_R}{1 + K_R^N n_R} \quad (3.48)$$

if there are m_R in total and K_R^N is the association constant for non-specific binding with n_R non-specific binding sites. For an activator

$$A \simeq \frac{m_A}{1 + K_A^N n_A} \quad (3.49)$$

with the parameters defined similarly.

With these expressions, we can add non-specific binding to any of the equations for transcriptional regulation we have already derived. Consider Eq. 3.15 for regulation by RNA polymerase and a repressor

$$\frac{dM}{dt} = \frac{nuK_Q Q}{1 + K_Q Q + K_R R} - d_M M. \quad (3.50)$$

This equation becomes

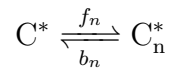
$$\frac{dM}{dt} = \frac{nuK_Q \cdot \frac{m_Q}{1 + K_Q^N n_Q}}{1 + K_Q \cdot \frac{m_Q}{1 + K_Q^N n_Q} + K_R \cdot \frac{m_R}{1 + K_R^N n_R}} - d_M M \quad (3.51)$$

using Eq. 3.47 and Eq. 3.48. Non-specific binding affects transcription by reducing the number of available regulators, from m_Q for polymerase, decreasing transcription, and from m_R for the repressor, increasing transcription.

3.7 Modelling signal transduction V

We can now add to the model of Sec. 2.12 the expression of the reporter gene in Fig. 1, which C^* activates.

The nuclear entry and exit of C^* can be written as a chemical reaction:



which, if at equilibrium, implies that

$$[C_n^*] = \frac{f_n}{b_n} [C^*]. \quad (3.52)$$

Making the simplest assumption that C_n^* is an activator that binds to a single binding site on the reporter gene, G , then the mRNA of G , m_G , satisfies, following Eq. 3.23,

$$\frac{d[m_G]}{dt} = u_G \frac{\frac{[C_n^*]}{K_{C^*}}}{1 + \frac{[C_n^*]}{K_{C^*}}} - d_m [m_G] \quad (3.53)$$

with a maximal transcription rate of u_G and a degradation rate d_m of the mRNA. Following Eq. 3.18, the protein G obeys

$$\frac{d[G]}{dt} = v [m_G] - d_G [G] \quad (3.54)$$

for translation rate v and degradation rate d_G of the protein G .

Eq. 2.100 with Eq. 3.53 and Eq. 3.54 are the complete model of the pathway of Fig. 1, from the input S to the output G .

4 Positive feedback and bistability

Positive feedback, where an increase in the output of a system causes the output of the system to increase further, can generate a bistable response. For certain parameter values, a system with positive feedback may have two stable steady states. If the system starts from one set of initial conditions and evolves with time, it will always eventually reach one steady state; if the same system starts from a different set of initial conditions, it will always eventually reach the other steady state. Each steady state has its own basin of attraction defined as all initial concentrations that evolve to that steady state, and each initial condition must lie in one of the two basins of attraction. Intuitively, if the level of output does not get sufficiently high then the system tends to one steady state; if the output gets high enough for the positive feedback to ‘run away’ and generate yet more output, then the system tends to the other steady state.

4.1 MAP kinase cascades: a one dimensional example

Understanding how positive feedback generates multiple steady states is best understood graphically. Consider the MAP kinase cascade in frog oocytes: activating the last kinase of the cascade by adding the hormone progesterone causes new synthesis of the MAP kinase kinase kinase Mos. There is thus positive feedback: more activated Mos causes more activated MAP kinase, which in turn generates more activated Mos by increasing Mos’s synthesis.

Following Ferrell *et al.* [13], we consider three processes that control levels of Mos. First, there is a basal rate of synthesis that depends on progesterone:

$$\text{basal synthesis} = k_b[p] \tag{4.1}$$

where k_b is the basal rate and $[p]$ is the concentration of progesterone. Second, positive feedback occurs because synthesis of Mos is proportional to the concentration of activated MAP kinase. If we assume that the concentration of MAP kinase is a Hill function of the concentration of Mos, then this term is:

$$\text{positive feedback} = f \frac{[\text{Mos}]^n}{K^n + [\text{Mos}]^n} \tag{4.2}$$

where f measures the strength of the feedback. Finally, Mos degrades, which we model as a first order process:

$$\text{degradation} = -[\text{Mos}] \tag{4.3}$$

measuring units of time in units of the lifetime of Mos so that the coefficient of $[\text{Mos}]$ is one.

Consequently, the rate of change of the concentration of Mos is

$$\frac{d[\text{Mos}]}{dt} = k_b[p] + f \frac{[\text{Mos}]^n}{K^n + [\text{Mos}]^n} - [\text{Mos}]. \tag{4.4}$$

Typical parameter values are $K = 20$ nM, $n = 5$, $k_b = 0.2$, and $f = 40$ [13].

At steady state, the rate of synthesis of Mos equals its rate of degradation. Therefore to find steady-state values, we can plot the total synthesis rate and the total degradation rate both as a function of Mos with any intersections between these two curves determining a steady-state concentration of Mos (Fig. 4A). Notice that if the rate of synthesis of Mos is not ultrasensitive but hyperbolic, then the system would have only one stable steady state and no switch-like behaviour (Fig. 4B).

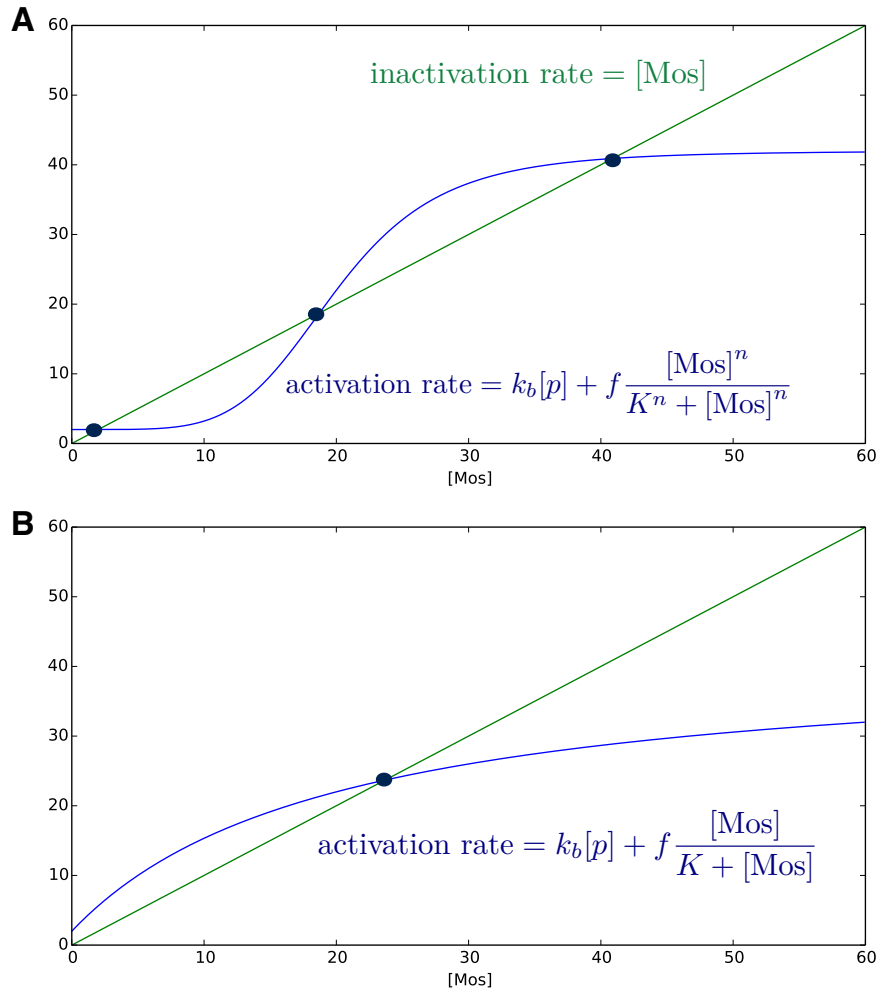


Figure 4: We can find steady-state solutions of Eq. 4.4 using a graphical construction: the intersection of a curve describing the production rate of $[\text{Mos}]$ with a curve describing its degradation rate gives the steady-state $[\text{Mos}]$ concentration. **A:** With a sigmoidal production rate, three steady states exist of which two are stable. **B:** With a hyperbolic production rate, there is only one steady state.

Depending on the initial conditions, the system will tend to one of the two steady states. It will avoid the unstable steady state. Even if the system initiates at the concentrations of the unstable steady state, any perturbation, no matter how small, will cause the system to tend to one of the two steady states (Fig. 5).



Figure 5: The phase portrait when $[p] = 20 \text{ nM}$ (see Fig. 6). If the initial $[\text{Mos}]$ is above the value at the unstable steady state, then $[\text{Mos}]$ tends to the upper stable steady state. If the initial $[\text{Mos}]$ is below the value at the unstable steady state, then $[\text{Mos}]$ tends to the lower stable steady state.

A bifurcation is a qualitative change in the dynamics of a system [14]. As we change the concentration of pheromone from, for example, low to high values, the number of steady-state concentrations of Mos changes from three to one (Fig. 6). This change in pheromone qualitatively changes the system’s dynamics: there has been a bifurcation.

When the system has one steady state then this steady state is stable (for example, when $[p] = 60$ nM), and the evolution of the system over time from any initial condition will ultimately lead to that steady state. When the system has three steady states (for example, when $[p] = 20$ nM), two steady states are stable and the steady state between these two steady states is unstable.

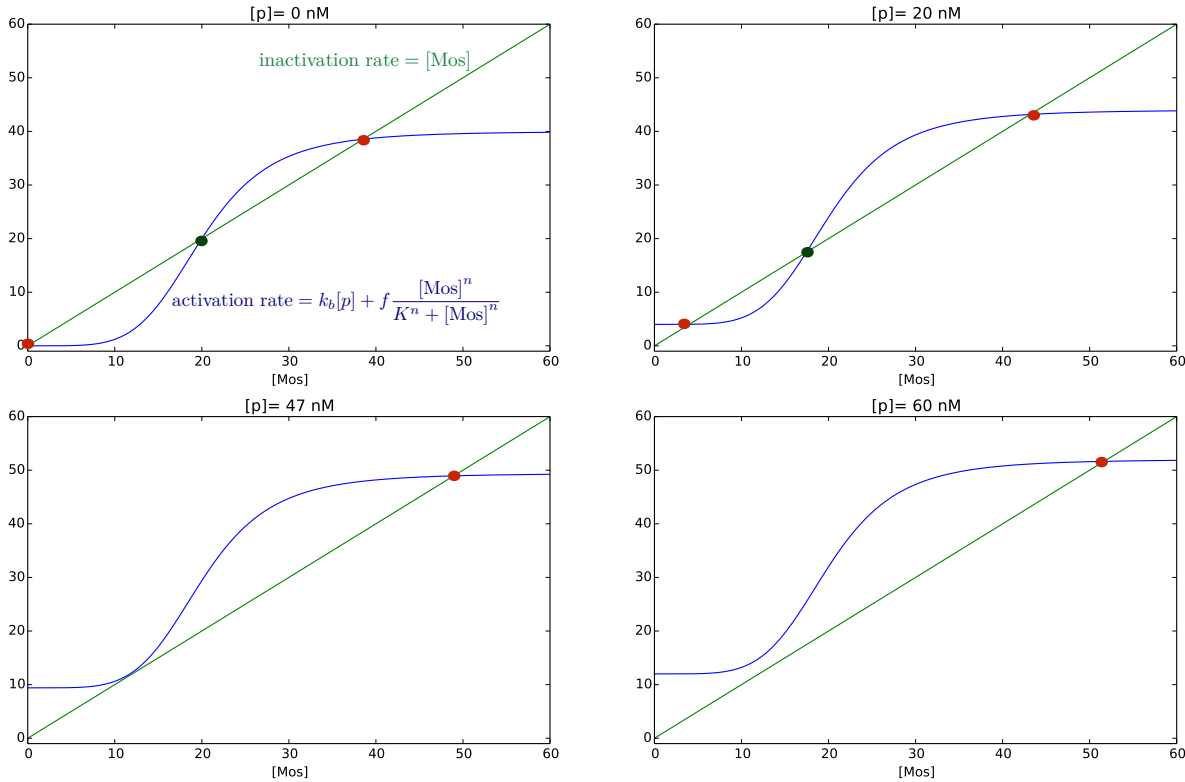


Figure 6: The number of stable steady states, denoted in red, changes as the concentration of pheromone changes, which determines the intercept with the y -axis.

As the concentration of pheromone increases from zero, one stable and the unstable steady state approach each other. At the bifurcation point, one ‘annihilates’ the other, and both disappear (at $[p] \simeq 47$ nM). The system then has only one steady state. We call this disappearance of a stable and an unstable steady state a saddle-node bifurcation [14]. Such a bifurcation can also create a stable and an unstable node if, for example, pheromone now decreases.

4.2 Bifurcation diagrams and hysteresis

A bifurcation diagram shows qualitative changes in the long-term behaviour of the output of a system as a function of a system parameter. For the MAPK system, we can plot the steady-state values of protein as a function of the progesterone concentration $[p]$ (Fig. 7).

For low $[p]$, there are two stable steady states for Mos (Fig. 6); for high $[p]$ there is one steady state (Fig. 6). Usually we mark stable steady states on bifurcation diagrams with solid lines and unstable steady states with fainter lines. The signalling system can therefore act as a switch with the steady-state concentration of Mos jumping from a low to a high value as the bifurcation parameter – here $[p]$ – changes.

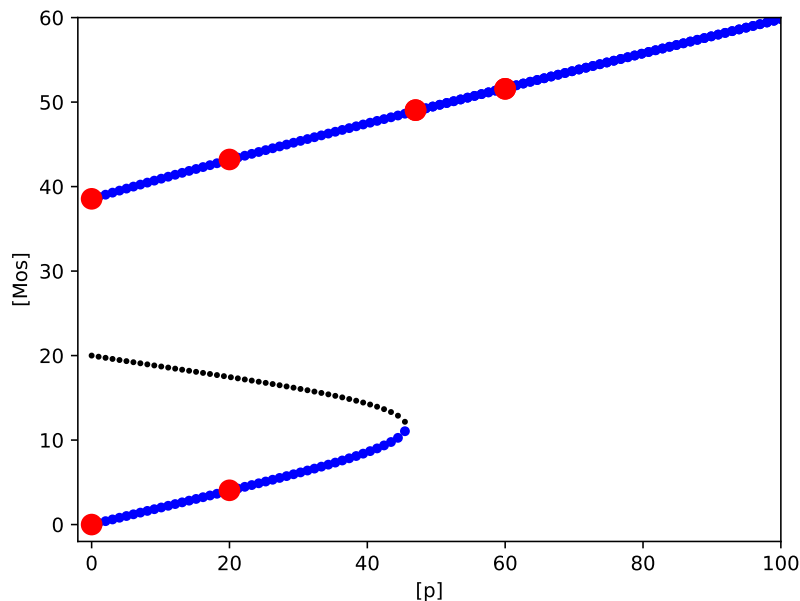


Figure 7: A bifurcation diagram showing the steady-state concentrations of Mos as a function of the concentration of pheromone. Stable steady states are in either blue or red; unstable steady states are in black. A saddle-node bifurcation occurs at $[p] \simeq 47$ nM. The stable steady states of Fig. 6 are in red.

Bistable systems typically show history-dependent, or hysteretic, behaviour. If we increase $[p]$ from low to high values, the steady-state level of $[Mos]$ jumps from a low to a high value at a particular threshold value of $[p]$, when the system goes through a saddle-node bifurcation. Decreasing $[p]$ will, in this example, cause no jump back to the low state of Mos, and the system has a permanent memory, always remembering its exposure to the high progesterone concentration.

Next we will consider a system that has the potential for not one but two saddle-node bifurcations.

4.3 A genetic switch: a two dimensional example of a saddle-node bifurcation

In systems with more than one chemical species, bistability and saddle-node bifurcations occur analogously to the one dimensional case.

For example, consider a protein that activates its own expression [14]. Writing M for mRNA and P for protein, we can model this two dimensional system as

$$\frac{dM}{dt} = u_b + \frac{uP^n}{K^n + P^n} - d_M M \quad ; \quad \frac{dP}{dt} = M - d_P P \quad (4.5)$$

with a Hill function describing the activation of transcription by P . Here d_M is the rate of degradation of mRNA; d_P is the rate of degradation of protein; u is the maximal rate of transcription induced by P ; and u_b is a basal rate of transcription. The system has positive feedback because high levels of protein cause higher rates of transcription and so even higher levels of protein.

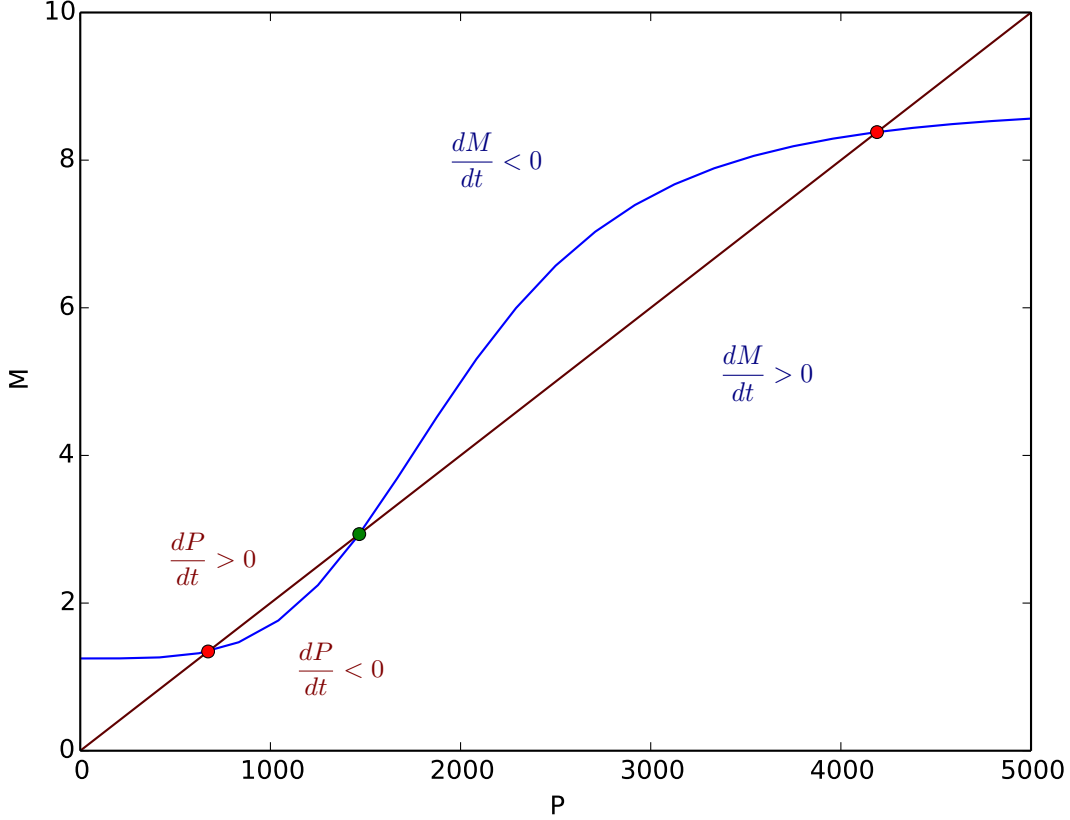


Figure 8: The intersection of the nullclines show the steady states of the model of the genetic switch. Stable steady states are in red; unstable steady states are in green. Here $n = 4$, $u_b = 0.01 \text{ s}^{-1}$, $d_M = 0.008 \text{ s}^{-1}$, $d_P = 0.002 \text{ s}^{-1}$, $K = 2000$, and $u = 0.06 \text{ s}^{-1}$.

In two dimensions, we often use graphical approaches to analyse bistable systems. At steady state, both dM/dt and dP/dt are zero. To find the possible steady states of the system, we plot the nullclines, defined as the curves where either dM/dt or dP/dt are zero [14]. These curves are

$$M = \frac{1}{d_M} \left(u_b + \frac{uP^n}{K^n + P^n} \right) \quad ; \quad M = d_P P \quad (4.6)$$

from Eq. 4.5, and we plot both curves in the same P - M plane (Fig. 8). The steady states are the points where the nullclines intercept: at these points, dM/dt and dP/dt are both zero.

The genetic switch of Fig. 8 has three steady states. The middle steady state is unstable; the other two steady states are stable. The stable states are called stable nodes because they are attracting: a system starting near a stable node will move over time towards the node. The unstable steady state is called a saddle point: a system near the saddle point is either immediately repelled from or initially attracted towards and then repelled from the saddle point. An unstable node in contrast repels all systems that are initialised sufficiently near it.

A phase portrait shows graphically the dynamics of the system. From Eq. 4.5, dM/dt is negative above the $dM/dt = 0$ nullcline, and the dynamics there decreases M ; dM/dt is positive below the $dM/dt = 0$ nullcline, and the dynamics there increases M (Fig. 8). Similarly, dP/dt is positive above the $dP/dt = 0$ nullcline, and the dynamics increases P ; dP/dt is negative below the $dP/dt = 0$ nullcline, and the dynamics decreases P . Using arrows to indicate the local direction of the dynamics, we can find the phase portrait (Fig. 9).

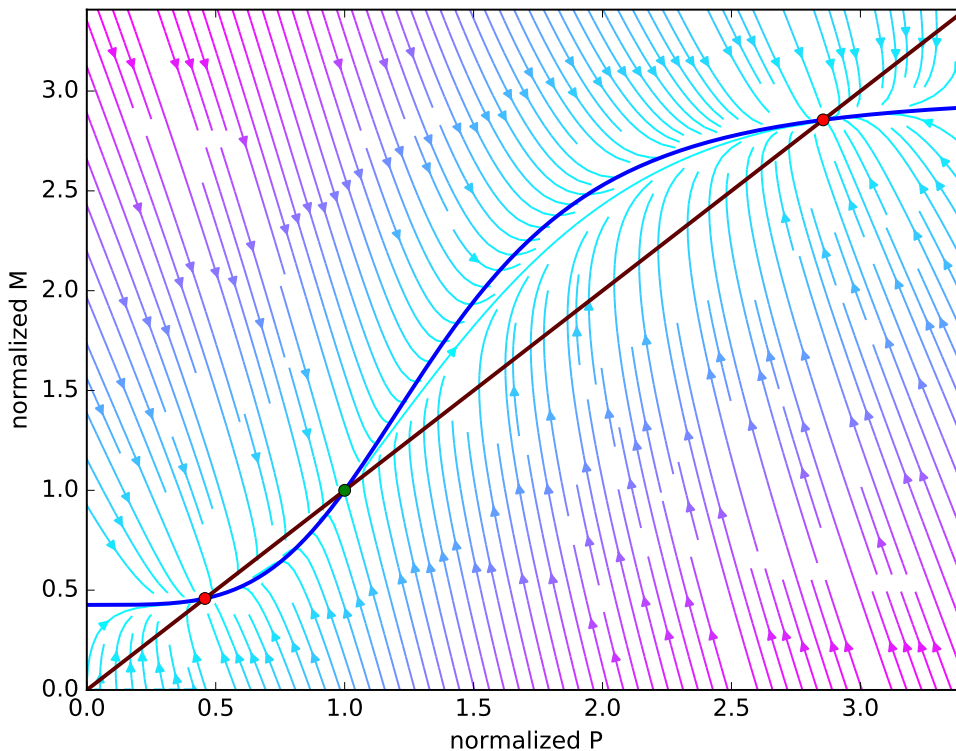


Figure 9: The phase portrait for the genetic switch shows two stable steady states in red separated by an unstable steady state in green. Protein and mRNA are relative to their levels at the unstable steady state.

As we change the degradation rate of protein, d_P , the system undergoes two saddle-node bifurcations. The number of intersections of the nullclines changes from one to three to one (Fig. 10). As we change d_P , a stable steady state, the node, and an unstable steady state, the saddle, either can approach and annihilate each other and thus remove bistability or can be simultaneously created and thus generate bistability. When the rescaled $d_P \simeq 0.8$, a saddle and a node appear if d_P is increasing and disappear if d_P is decreasing. Similarly, when the rescaled $d_P \simeq 1.3$, a node and a saddle point disappear if d_P is increasing and appear if d_P is decreasing (Fig. 10). Saddle-node bifurcations can create and destroy bistability in all dimensions.

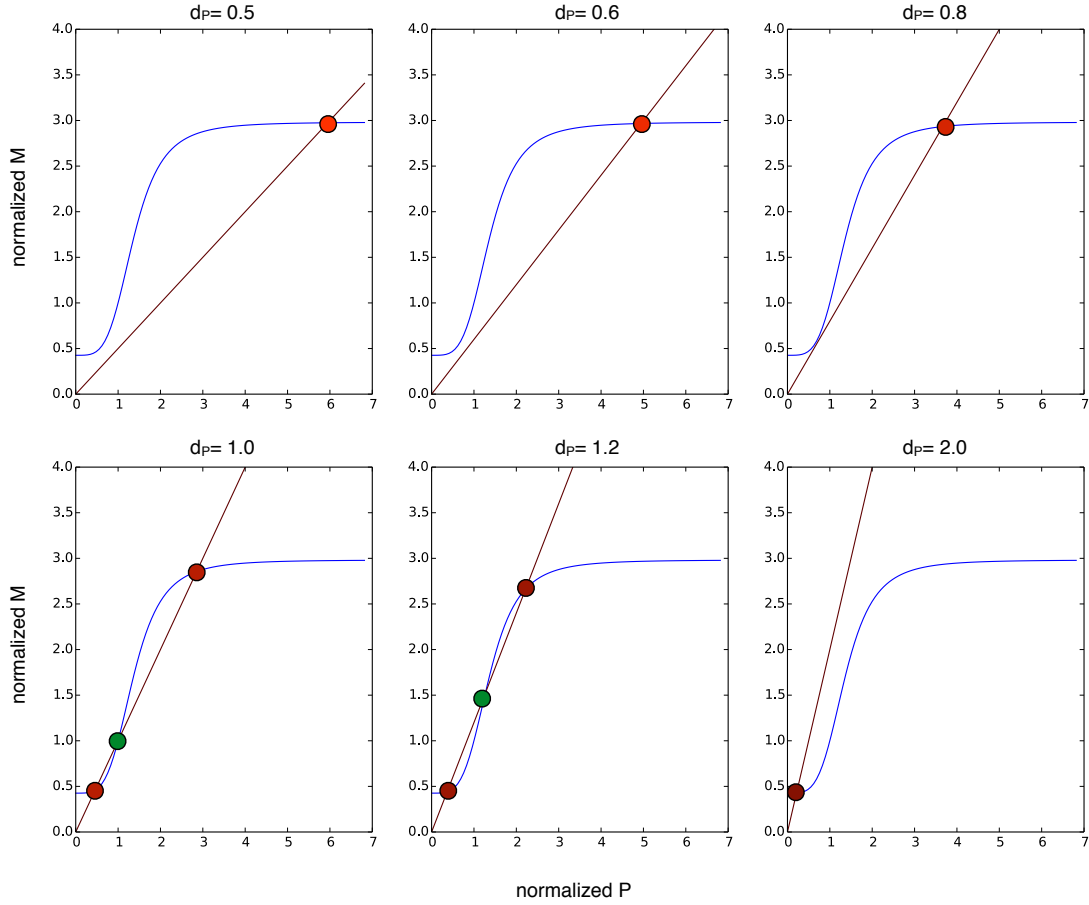


Figure 10: When we change d_p , the system undergoes two saddle-node bifurcations: one at the rescaled $d_P \simeq 0.8$ and the other at $d_P \simeq 1.3$ (not shown). Protein and mRNA are relative to their levels at the unstable steady state when $d_P = 0.002 \text{ s}^{-1}$, and we measure d_P relative to 0.002 s^{-1} .

The system exhibits hysteresis, or history-dependent behaviour. If we increase d_P from low values, the system jumps from a high value of P to a low value at the bifurcation, when the rescaled $d_P \simeq 1.3$ (Fig. 11). If we decrease d_P from high values, the system jumps from a low value of P to a high value at the bifurcation when the rescaled $d_P \simeq 0.8$ (Fig. 11). The value of the threshold when the jump occurs depends on the history of the change in d_P .

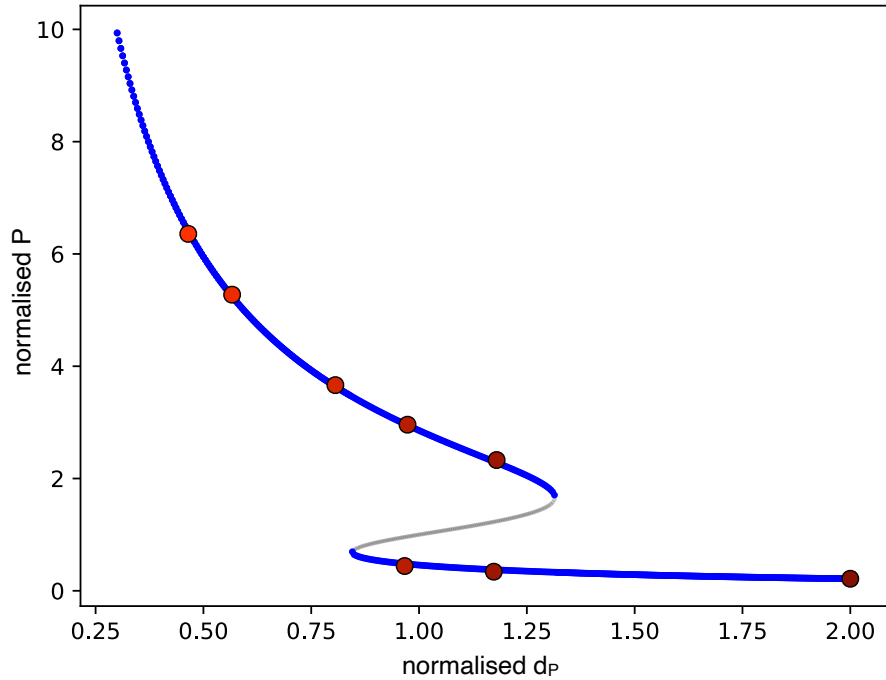


Figure 11: The bifurcation diagram for the genetic switch. The stable steady states are in blue and the unstable steady states in grey. The stable-steady states of Fig. 10 are in shades of red. Protein and mRNA are relative to their levels at the unstable steady state when $d_P = 0.002 \text{ s}^{-1}$, and we measure d_P relative to 0.002 s^{-1} .

This behaviour is general. A system with positive feedback can exhibit hysteresis because the value of the bifurcation parameter at which the system jumps — undergoes a bifurcation — is history-dependent: if the system was previously in the high state, then the threshold value at the bifurcation is different from the threshold value if the system was previously in the low state. Observing hysteresis experimentally is usually considered sufficient proof that a system is bistable; observing bimodality, however, is consistent with bistability but insufficient to prove bistability.

5 Negative feedback and oscillations

A limit cycle is an isolated and closed trajectory in phase space [14]. Remember that phase space is the space where we plot the concentration of each chemical species along each axis. An isolated trajectory means that neighbouring trajectories either spiral towards the closed trajectory or spiral away from it. Once on a stable limit cycle, the system continues to move around the cycle: the concentrations of the chemical species continually revisit values they have had before, and the system oscillates.

5.1 Degradation stabilises molecular numbers

Degradation stabilises protein numbers. Consider a protein P with constitutive expression

$$\frac{dP}{dt} = k - d_P P. \quad (5.1)$$

Then at steady state when $P = P^*$ the rate of synthesis, k , exactly equals the rate of degradation

$$k = d_P P^*. \quad (5.2)$$

If levels of P fluctuate higher than P^* , then the rate of synthesis is unchanged but the rate of degradation increases, $d_P P > d_P P^* = k$, so that degradation dominates synthesis. Degradation therefore returns the levels of proteins to their steady-state levels. Similarly, if levels of P fluctuate lower than P^* , then the rate of degradation decreases, $d_P P < d_P P^* = k$, allowing synthesis to dominate and protein levels to regain steady state.

5.2 Negative feedback is stabilising

Negative feedback acts to reduce perturbations to a system, providing an additional restoring process to degradation.

Consider a gene that is negatively auto-regulated by its protein P so that

$$\frac{dP}{dt} = \frac{k}{1 + (P/K)^n} - d_P P \quad (5.3)$$

where we use a Hill function to describe the auto-regulation. This negative regulation generates negative feedback in the system. At steady state, $P = P^*$ and

$$\frac{k}{1 + (P^*/K)^n} = d_P P^* \quad (5.4)$$

so that the rate of synthesis of P equals its rate of degradation.

If levels of P fluctuate higher than P^* , then

$$\frac{k}{1 + (P/K)^n} < \frac{k}{1 + (P^*/K)^n}. \quad (5.5)$$

The auto-negative regulation increases repression, decreasing the synthesis rate, because there are more proteins to bind P 's promoter. Levels of P fall towards P^* . If levels of P fluctuate lower than P^* , then

$$\frac{k}{1 + (P/K)^n} > \frac{k}{1 + (P^*/K)^n}. \quad (5.6)$$

The repression lessens, increasing the synthesis rate, because there are fewer proteins to bind the promoter. Levels of P rise towards P^* .

5.3 Delayed negative feedback can cause oscillations

Delayed negative feedback can be destabilising and generate oscillations providing both the feedback is sufficiently strong and the delay is sufficiently long.

Consider again a negatively auto-regulated gene. At steady state, the synthesis rate exactly matches the degradation rate. If levels of protein fluctuate above average levels, synthesis falls because repression increases. If the fall in synthesis is delayed, however, then levels of protein will rise higher than those for a system without a delay. Once levels of protein do return to the average, there is a mismatch between the current levels of protein and the synthesis rate. This synthesis rate is determined by the higher levels of protein that existed earlier, because of the delay. Synthesis is therefore too low compared to the current rate of degradation, which is determined by the current levels of protein. Protein levels do not stay at the average, but undershoot it. After undershooting, levels of proteins will eventually start to increase and return towards the average, but when they reach the average the synthesis rate will again not match the degradation rate. Now the lower levels of protein that existed earlier determine the synthesis rate, and synthesis is too high compared to degradation. Protein levels overshoot the average, and a cycle initiates. The delays in negative feedback cause protein levels to alternatively undershoot and overshoot their average level; the system oscillates.

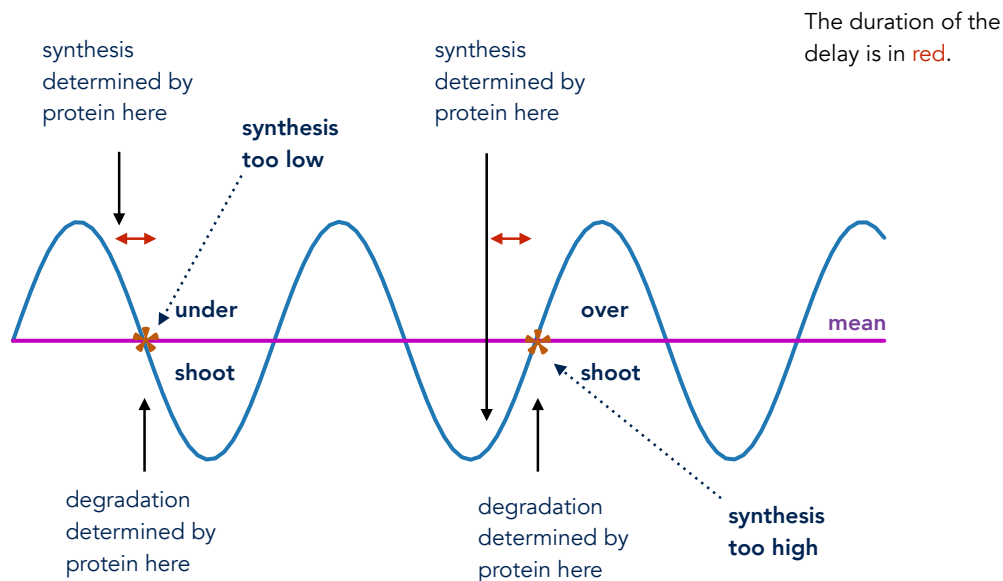


Figure 12: Negative feedback can cause oscillations in the levels of proteins (blue) of a negatively auto-regulated gene if the negative feedback is sufficiently strong and sufficiently delayed. When proteins reach their average level (asterisks), the delay causes a mismatch between the synthesis rate and the degradation rate so that the levels of protein continually undershoot and overshoot – they oscillate.

5.4 Circadian rhythms

Circadian rhythms are free-running oscillations generated by biochemical networks within single cells. By free-running, we mean they can exist in the absence of cues from the earth's 24 hour cycle. Circadian rhythms have a period of approximately 24 hours and can be synchronised by

environmental signals, such as light and temperature. They are also temperature compensated, persisting over a range of temperatures.

Researchers have studied circadian rhythms in *Drosophila*, and Konopka and Benzer discovered the first mutation to disrupt the circadian rhythm. This mutation was in the *period* or *per* gene.

In *Drosophila*, the basis of the circadian rhythm is delayed negative feedback through negative auto-regulation of the *per* gene by the PER protein. After transcription, PER proteins accumulate in the cytoplasm and re-enter the nucleus only after a delay to repress transcription of *per*. A kinase called DBT (double-time) phosphorylates PER in the cytoplasm, and this phosphorylation is necessary for PER's degradation. PER can, however, exist as both a monomer and a dimer. Although DBT phosphorylates both, only the dimer represses the *per* gene.

We will follow the model of Tyson *et al.* [15] (Fig. 13) to explore how the genetic network in *Drosophila* generates oscillations. Tyson *et al.* assume that the PER dimer rapidly equilibrates between the cytoplasm and the nucleus and that the interconversion of PER monomers and dimers is also at equilibrium.

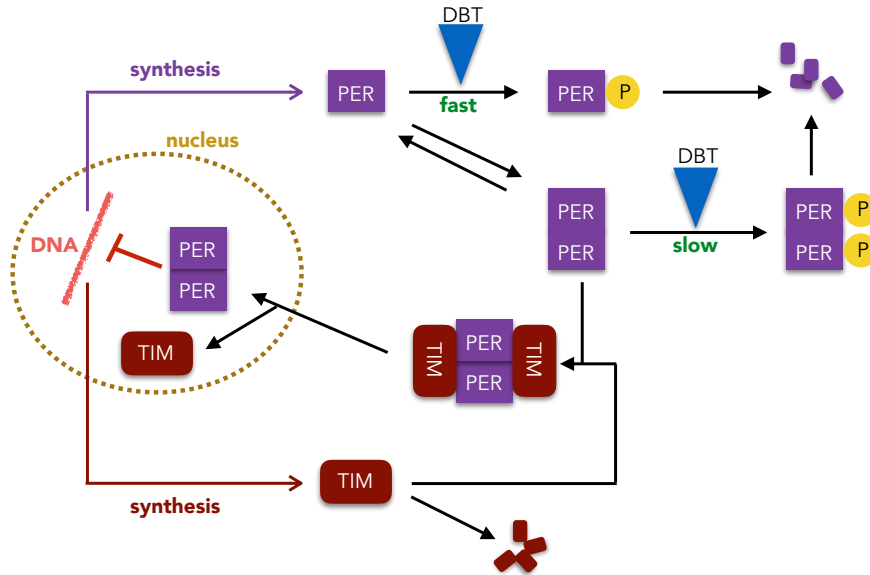
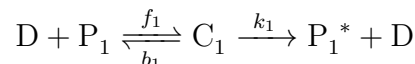


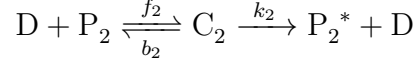
Figure 13: The model of circadian rhythms of Tyson *et al.* involves a delayed negative feedback where the transcription factor PER represses its own expression when it is a dimer and when it is imported into the nucleus in a complex with TIM. Tyson *et al.* choose not to model TIM explicitly, but include its effects by having different rates of degradation of PER monomers and dimers by DBT.

5.4.1 Competitive inhibition

First we will investigate the rate of phosphorylation of DBT, which is an enzyme that has two substrates: PER monomers and PER dimers. Assuming that both phosphorylations proceed with Michaelis-Menten reactions and, denoting P_1 for PER monomers and P_2 for PER dimers, we have



and



where we use D to denote the kinase DBT.

As before (see Eq. 2.87), we assume that both C_1 and C_2 , the kinase-substrate complexes, are at quasi-steady state. Then

$$\begin{aligned} \frac{dC_1}{dt} &= f_1DP_1 - (b_1 + k_1)C_1 \simeq 0 \\ \frac{dC_2}{dt} &= f_2DP_2 - (b_2 + k_2)C_2 \simeq 0 \end{aligned} \quad (5.7)$$

and therefore

$$C_1 \simeq \frac{f_1DP_1}{b_1+k_1} \quad ; \quad C_2 \simeq \frac{f_2DP_2}{b_2+k_2}. \quad (5.8)$$

The total amount of kinase, D_T , is fixed, and $D + C_1 + C_2 = D_T$. This conservation law and Eq. 5.8 implies that

$$D = \frac{D_T}{1 + \frac{f_1P_1}{b_1+k_1} + \frac{f_2P_2}{b_2+k_2}}. \quad (5.9)$$

Consequently, the rate of formation of P_1^* , which is k_1C_1 , equals

$$k_1 \times \frac{f_1P_1}{b_1+k_1} \times \frac{D_T}{1 + \frac{f_1P_1}{b_1+k_1} + \frac{f_2P_2}{b_2+k_2}} \quad (5.10)$$

using Eq. 5.8 and Eq. 5.9. We can thus write

$$\frac{dP_1^*}{dt} = \frac{k_1D_TP_1}{\frac{b_1+k_1}{f_1} + P_1 + \frac{f_2(b_1+k_1)}{f_1(b_2+k_2)}P_2} \quad (5.11)$$

and similarly can show that the rate of formation of P_2^* is

$$\frac{dP_2^*}{dt} = \frac{k_2D_TP_2}{\frac{b_2+k_2}{f_2} + P_2 + \frac{f_1(b_2+k_2)}{f_2(b_1+k_1)}P_1}. \quad (5.12)$$

PER dimers therefore inhibit the phosphorylation of PER monomers – high P_2 decreases dP_1^*/dt , and PER monomers inhibit the phosphorylation of PER dimers – high P_1 decreases dP_2^*/dt . Both isoforms competitively inhibit the phosphorylation of the other by sequestering the enzyme DBT.

If the Michaelis-Menten constant of DBT is the same for both substrates, so that $\frac{b_1+k_1}{f_1} = \frac{b_2+k_2}{f_2} = K$ say, then

$$\begin{aligned} \frac{dP_1^*}{dt} &= \frac{V_1P_1}{K + P_1 + P_2} \\ \frac{dP_2^*}{dt} &= \frac{V_2P_2}{K + P_1 + P_2} \end{aligned} \quad (5.13)$$

with $V_1 = k_1D_T$ and $V_2 = k_2D_T$. Eq. 5.13 is the form used by Tyson *et al.* [15].

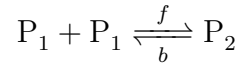
5.4.2 The Tyson *et al.* model

Tyson *et al.* have three equations in their model: one for *per* mRNA, one for PER monomers, and one for PER dimers. They use a Hill function with a Hill number of two to model negative auto-regulation of *per* expression by PER dimers. The equation for *per* mRNA levels is then

$$\frac{dM}{dt} = \frac{u}{1 + \left(\frac{P_2}{P_c}\right)^2} - d_M M \quad (5.14)$$

with d_M being the rate of degradation of mRNA.

PER monomers are translated from the mRNA with rate v , phosphorylated by DBT, actively degraded at rate d_p , and undergo dimerisation



so that

$$\frac{dP_1}{dt} = vM - \frac{V_1 P_1}{K + P_1 + P_2} - d_P P_1 - 2fP_1^2 + 2bP_2 \quad (5.15)$$

using Eq. 5.13. Once phosphorylated, the PER monomers rapidly degrade and no longer contribute to the dynamics.

PER dimers also undergo phosphorylation, degradation, and monomerisation:

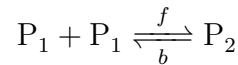
$$\frac{dP_2}{dt} = -\frac{V_2 P_2}{K + P_1 + P_2} - d_P P_2 + fP_1^2 - bP_2. \quad (5.16)$$

Once phosphorylated, the PER dimers degrade too.

By assuming equilibrium between PER monomers and dimers, Tyson *et al.* were able to reduce this system of three equations to two equations.

5.4.3 Dimerisation

The dimerisation reaction of PER proteins is



and so at equilibrium

$$P_2 = \frac{f}{b} P_1^2. \quad (5.17)$$

If we write the total number of PER monomers, both free and in dimers, as P_T , where P_T can change with time, then

$$P_T = P_1 + 2P_2 \quad (5.18)$$

and so

$$P_T = P_1 + 2\frac{f}{b} P_1^2 \quad (5.19)$$

which is a quadratic equation for P_1 :

$$P_1^2 + \frac{b}{2f} P_1 - \frac{b}{2f} P_T = 0. \quad (5.20)$$

We can solve this equation following the usual formula

$$\begin{aligned}
 P_1 &= \frac{-1 + \sqrt{1 + 8\frac{f}{b}P_T}}{4\frac{f}{b}} \\
 &= \frac{2P_T}{1 + \sqrt{1 + 8\frac{f}{b}P_T}}
 \end{aligned}
 \tag{5.21}$$

where we have multiplied both top and bottom by $2/q$ with q being

$$q = \frac{2}{1 + \sqrt{1 + 8\frac{f}{b}P_T}}.
 \tag{5.22}$$

Consequently the equilibrium concentrations both have a convenient form as functions of P_T :

$$P_1 = qP_T \quad ; \quad P_2 = \frac{1}{2}(1 - q)P_T
 \tag{5.23}$$

with q given by Eq. 5.22.

5.4.4 The final model with two rate equations

By adding dP_1/dt to twice dP_2/dt , Tyson *et al.* find a differential equation for $P_T = P_1 + 2P_2$:

$$\frac{dP_T}{dt} = vM - \frac{V_1q + V_2(1 - q)}{K + \frac{1}{2}(1 + q)P_T}P_T - d_P P_T
 \tag{5.24}$$

using Eq. 5.23, which replaces Eq. 5.15 and Eq. 5.16.

Similarly we use Eq. 5.23 to write Eq. 5.14 in terms of P_T rather than P_2 :

$$\frac{dM}{dt} = \frac{u}{1 + \frac{(1-q)^2P_T^2}{4P_2^2}} - d_M M
 \tag{5.25}$$

with q obeying Eq. 5.22.

With now two variables, P_T and M , we can investigate the dynamics, Eq. 5.24 and Eq. 5.25, using phase plane analysis. The nullclines intersect at one point, but this point is unstable for certain values of the parameters [15], and the system oscillates.

The system has negative feedback because of the repression of the *per* gene by PER dimers, and this feedback is delayed because cells must synthesise PER and then convert it into dimers before it represses transcription. The delayed negative feedback drives the circadian oscillations.

The system also has positive feedback. If the number of dimers is sufficiently high that the rate of phosphorylation of dimers by DBT saturates, then an increase in the number of dimers cannot affect the rate of phosphorylation of dimers, but does still decrease the rate of phosphorylation of PER monomers. PER monomers consequently build up and so too do PER dimers because of the equilibrium existing between monomers and dimers. An increase in PER dimers therefore generates a further increase in dimers – the system has positive feedback. Positive feedback is strongest for dimers rather than monomers because monomers are more rapidly phosphorylated by DBT, $V_2 \ll V_1$. The positive feedback allows PER dimers to increase quickly once their numbers become sufficiently high.

5.5 Relaxation oscillations

Systems with both positive and negative feedback can undergo relaxation oscillations. A relaxation oscillation has a slow buildup, where we can think of ‘stress’ accumulating, and then a fast ‘discharge’, where the stress dissipates. The system must therefore have two widely separated time scales [14].

The Tyson *et al.* model has positive and negative feedback and both slow and fast times scales. It exhibits relaxation oscillations. The increase of the numbers of PER dimers generates a slow time scale. This process is slow because mRNA must first be synthesised and then translated and because PER monomers are rapidly degraded by DBT ($V_1 \gg V_2$ in Eq. 5.14 and Eq. 5.15). The decrease in the number of PER dimers once they repress transcription of *per* generates the fast time scale. The number of PER dimers quickly falls despite DBT preferentially degrading monomers because the loss of monomers causes the PER dimers to dissociate to maintain the dimer-monomer equilibrium.

5.6 Oscillations through both positive and negative feedback

Oscillators with both positive and negative feedback are typically built around an underlying bistable system, although one that only exists if there is no negative feedback. For example, if there is no repression of *per* transcription by PER dimers in the Tyson *et al.* model then the system no longer oscillates and has two stable steady states. Tyson *et al.* postulate that the circadian oscillator may have evolved from a bistable system, which switches ‘on’ with dawn and ‘off’ with dusk via a component of the network regulated by light. They suggest the dissociation constant for PER’s dimerisation [15]. A clock improves on a switch because the cell can prepare for the day in advance without needing activation by light.

With both positive and negative feedback, the limit cycle driving the oscillations is often built around a hysteretic loop that would be generated by the positive feedback acting alone. Negative feedback prevents bistability and causes the system to oscillate, but the properties of the oscillations are still determined by the former hysteretic loop. The dynamics may be slow when the concentrations of the oscillating species are near the former steady-state values of the bistable system and will be fast when the concentrations of the oscillating species are moving between these values. The difference in concentrations between the two former steady states approximately determines the amplitude of the oscillations, and the time taken by the system to move around the loop determines their period.

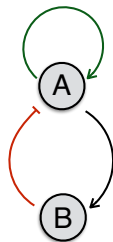
Such relaxation oscillators can have an amplitude and frequency that are robust to stochastic fluctuations [16]. The amplitude is more robust because it is determined by the stable fixed points of the former bistability [16, 17]. The period is more robust at least to stochastic effects if the magnitude of the stochastic fluctuations tend to be higher when the oscillator is moving quickly. Then this noisy section of the oscillator’s orbit is short-lived and contributes little to the period. Indeed, the circadian oscillator does moves faster when numbers of molecules are lower [18].

The former stable steady states also allow dual feedback oscillators to tune the frequency of the oscillations while maintaining their amplitude [17]. Such behaviour is, for example, important for the effective functioning of the human heart. As the frequency changes, the former steady states need not. For most systems, however, the limit cycle of the oscillations does not completely follow the former hysteretic loop, and so the amplitude can change as the frequency changes. Usually this change is smaller, however, than the equivalent change in amplitude for an oscillator

built from negative feedback alone [17].

5.6.1 Understanding a dual feedback oscillator

To understand better the role of the negative feedback in a dual feedback oscillator, consider a two-gene example: gene A is positively auto-regulated and activates a second gene B whose protein product represses gene A's transcription [19]. The auto-regulation generates positive feedback on gene A's expression; the repression through B generates negative feedback.



Modelling the positive feedback: Consider first the positive feedback. From Sec. 3.4, an equation describing the transcription of gene A is

$$\frac{dM}{dt} = \frac{u_{\text{basal}} + u_{\text{max}} \frac{A^2}{K_A^2}}{1 + \frac{A^2}{K_A^2}} - d_M M \quad (5.26)$$

where we include a basal rate and, to make things simpler, assume that a second protein A quickly binds the promoter once one binds, giving the denominator a term proportional to protein A^2 but no term proportional to A — compare with Eq. 3.35. There is positive feedback because more protein A increase the rate of transcription causing more protein A to be synthesised. For translation, we again have Eq. 3.8,

$$\frac{dA}{dt} = vM - d_A A. \quad (5.27)$$

If the reactions controlling levels of mRNA are much faster than those controlling levels of protein, we can then approximate Eq. 5.26 as being at quasi-steady state: $dM/dt = 0$. Solving for M , Eq. 5.27 then becomes

$$\frac{dA}{dt} = \frac{v}{d_M} \left[\frac{u_{\text{basal}} + u_{\text{max}} \frac{A^2}{K_A^2}}{1 + \frac{A^2}{K_A^2}} \right] - d_A A. \quad (5.28)$$

Simplifying through re-scaling: We will use re-scaling to reduce the number of parameters. There are two natural scales in the system — a time scale set by $1/d_A$ and a concentration scale set by K_A . We re-scale by these two parameters to generate two dimensionless variables, $\tilde{t} = d_A t$ and $\tilde{A} = A/K_A$. Dividing Eq. 5.28 by K_A and by d_A , we can write

$$\frac{1}{d_A} \cdot \frac{d}{dt} \left(\frac{A}{K_A} \right) = \frac{v}{d_A d_M K_A} \left[\frac{u_{\text{basal}} + u_{\text{max}} \frac{A^2}{K_A^2}}{1 + \frac{A^2}{K_A^2}} \right] - \frac{A}{K_A} \quad (5.29)$$

or

$$\frac{d\tilde{A}}{d\tilde{t}} = \frac{v}{d_A d_M K_A} \left[\frac{u_{\text{basal}} + u_{\text{max}} \tilde{A}^2}{1 + \tilde{A}^2} \right] - \tilde{A}. \quad (5.30)$$

Finally we will define $\alpha = \frac{v u_{\text{max}}}{d_A d_M K_A}$ and $b = u_{\text{basal}}/u_{\text{max}}$ giving

$$\frac{d\tilde{A}}{d\tilde{t}} = \alpha \left[\frac{b + \tilde{A}^2}{1 + \tilde{A}^2} \right] - \tilde{A}. \quad (5.31)$$

Comparing Eq. 5.31 and Eq. 5.28, the rescaling has decreased the number of parameters from six to two.

Adding negative feedback: To include negative feedback on gene A, we will let protein A activate gene B, and protein B repress gene A. No longer explicitly writing the tildes, but time is still in units of $1/d_A$ and concentration in units of K_A , we can write [19]

$$\begin{aligned} \frac{dA}{dt} &= \frac{\alpha [b + A^2]}{\left[1 + \left(\frac{B}{K}\right)^2\right] [1 + A^2]} - A \\ \frac{dB}{dt} &= \kappa A - d_B B. \end{aligned} \quad (5.32)$$

There are two simplifying assumptions. First, the binding sites of A and B are sufficiently far apart on the promoter of gene A that the two proteins do not interact: the equivalent of K_i in Eq. 3.38 is one so that the denominator in Eq. 5.32 factorises. Second, the rate of transcription of gene B is simply proportional to A : we model transcription just as in Eq. 3.23, but impose $A \ll K_1$.

Bistability for fixed B: Fixing B at a particular concentration, we'll show is equivalent to changing the value of α in Eq. 5.32. At steady state, $dA/dt = 0$ and so

$$\tilde{\alpha}(b + A^2) = A(1 + A^2) \quad (5.33)$$

where

$$\tilde{\alpha} = \frac{\alpha}{\left[1 + \left(\frac{B}{K}\right)^2\right]}. \quad (5.34)$$

Rearranging Eq. 5.33 gives

$$A^3 - \tilde{\alpha}A^2 + A - \tilde{\alpha}b = 0, \quad (5.35)$$

a cubic equation.

We will use Descartes's rule of signs to determine the number of positive solutions of Eq. 5.35. For a polynomial equation

$$x^n + a_{n-1}x^{n-1} + a_{n-2}x^{n-2} + \dots + a_1x + a_0 = 0, \quad (5.36)$$

Descartes showed that the maximum number of positive roots is equal to the number of changes of sign in the polynomial's coefficients moving from left to right [20]. Further, if there are N changes of sign, the number of positive routes is either N or $N - 2$ or $N - 4$, etc. For Eq. 5.35, we have three changes of sign and so either three positive roots – bistability – or one positive root – monostability (Fig. 14).

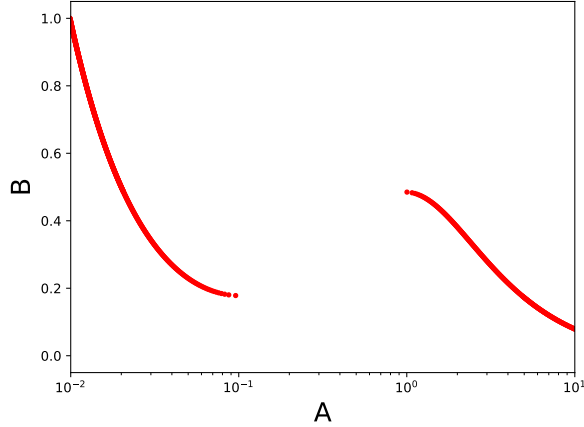


Figure 14: For intermediate, fixed values of B , the positive feedback generates two stable steady-state solutions for A . By changing B , we change $\tilde{\alpha}$ and so the solutions of Eq. 5.35. Here $\alpha = 50$, $b = 0.01$, $K = 0.02$, $d_B = 0.01$, and $\kappa = 0.8d_B$.

A limit cycle when B is not fixed: How B causes oscillations by de-stabilising A is easiest to understand when levels of B change slowly compared to levels of A [19]. Let $d_B \ll 1$ in Eq. 5.32 and let κ , which determines the time scale of B 's synthesis, be of the same size as d_B : $\kappa = \mathcal{O}(d_B)$. For example, $\kappa = 0.8d_B$ in Fig. 14. Then B responds slowly to changes in A , which moves quickly in comparison.

To generate oscillations in an anticlockwise direction around the bistable solutions in Fig. 14, we wish B to destabilise A when A is at the lower limit of the left branch in Fig. 14. A will then jump to the right branch. Similarly, B should also destabilise A when A reaches the upper limit of the right branch so that A jumps back to the left one.

When A is at the left branch's lower limit, the magnitude of the system's negative feedback should therefore be decreasing so that A 's rate of synthesis grows, favouring A moving to the right branch with its higher levels of A . To have decreasing negative feedback, levels of B should be falling so that there is less repression. Therefore we require $dB/dt < 0$ when A is at the left branch's lower limit.

When A is at the right branch's upper limit, the system's negative feedback should be increasing so that A 's rate of synthesis diminishes, favouring A moving to the left branch with its lower levels of A . Therefore we require $dB/dt > 0$ when A is at the right branch's upper limit so that levels of B are rising, generating more repression.

One way to impose these two conditions is to have the nullcline of B , where $dB/dt = 0$, pass between the two bistable solutions (Fig. 15A). To the nullcline's left, for smaller A , $dB/dt < 0$ from Eq. 5.32, and, to the nullcline's right, for larger A , $dB/dt > 0$, as we require. The negative feedback then destabilises the steady-state solutions, generating oscillations (Fig. 15A). If the nullcline intercepts the bistable solutions, however, there are no oscillations (Fig. 15B).

When A is near the former low steady states, the system moves slowly. There positive feedback is weak, and A 's synthesis rate is only slowly increasing as B slowly decreases. Eventually there is insufficient B to repress gene A , and levels of A quickly increase through positive feedback with A spiking and moving near the former high steady states. The now slowly increasing B and the high degradation rate of A quickly decrease levels of A . When levels are low enough

to weaken the positive feedback and B is sufficiently high to repress gene A , A moves quickly back to near the former low steady states. The positive feedback is then again weak and the negative feedback is strong because of the high levels of B . Levels of A change slowly once more.

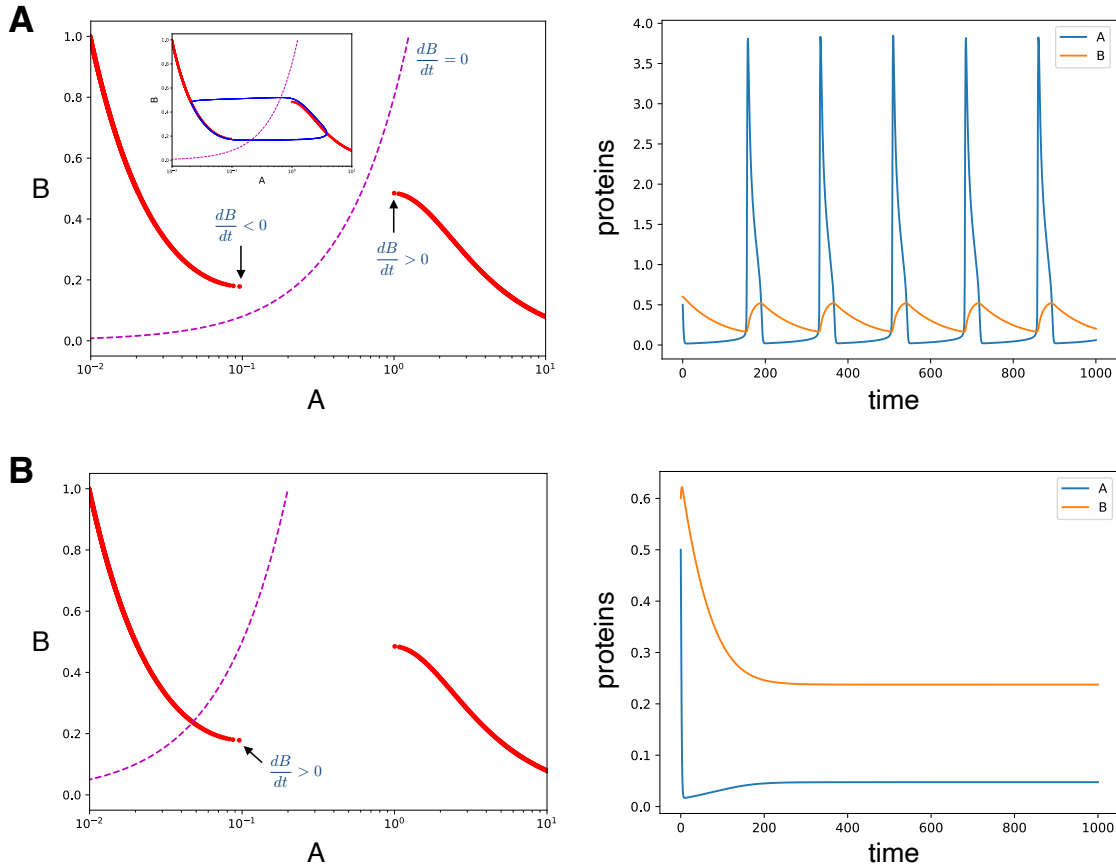


Figure 15: The negative feedback generates oscillations by destabilising the steady states. Here $\alpha = 50$, $b = 0.01$, $K = 0.02$, and $d_B = 0.01$, as before. **A** When $\kappa = 0.8d_B$, the nullcline of B passes between the branches of stable steady states that exist when B is fixed. The negative feedback therefore encourages A to jump from the left to the right branch when A and B are small and from the right to the left branch when A and B are large. The systems oscillates. The inset shows the limit cycle generated by the simulated time series in blue: with $d_B \ll 1$, the oscillations are around the former steady states generated by the positive feedback. **B** When $\kappa = 5d_B$, the nullcline of B does not pass between the two branches. At the lower limit of the left branch, when A and B are both small, B is increasing and so too is the magnitude of the negative feedback. A 's rate of synthesis is therefore falling, favouring A remaining near the former steady state with its low values of A . There are no oscillations.

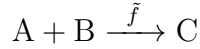
We can understand too some of the properties of the oscillations [19]. The difference in time scales describing A and B 's dynamics imposed by $d_B \ll 1$, or if we remove the re-scaling by $d_B \ll d_A$, generates relation oscillations. Levels of B change slowly, but levels of A spike when A quickly moves from near the former low steady states to near the former high steady states and then is rapidly degraded. The slow dynamics of B means that B principally determines the period, which increases as the time scale associated with B increases — when d_B decreases. The positive feedback determines the amplitude of the oscillations through the values of A at the former steady states: the size of the spikes in A is proportional to the distance between these

steady states.

Appendix A Simulating stochastic biochemical reactions

Often we use the Gillespie algorithm [1] to simulate fluctuations in biochemical systems. The computer “rolls” the equivalent of two dice: one to choose which reaction will occur next and the other to choose when that reaction will occur.

Consider a system in which n different reactions are possible, then we should first calculate the probability that each type of reaction will occur at the end of an interval of time t . Let this probability per unit time be $P_i(t)$ for reaction i . For example, if reaction i corresponds to the second-order reaction



then

$$\begin{aligned} P(\text{reaction } i \text{ in an interval } \delta t) &= N_A N_B \tilde{f} \delta t \\ &\equiv a_i \delta t \end{aligned}$$

where $a_i = N_A N_B \tilde{f}$ is referred to as reaction i 's propensity and δt is sufficiently small that only one reaction can occur. We can use Eq. A.1 to split the probability $P_i(t)\delta t$ into two events:

$$P_i(t)\delta t = P(\text{no reactions for time } t) \times P(\text{reaction } i \text{ in the interval } \delta t) \quad (\text{A.1})$$

and if we write $P_0(t)$ as the probability of no reactions occurring during an interval t , then

$$P_i(t)\delta t = P_0(t)a_i\delta t. \quad (\text{A.2})$$

To find $P_0(t)$, consider the probability of having no reactions during an interval $t + \delta t$, which is the product of the probability of having no reactions during t and the probability of no reactions occurring during δt :

$$P_0(t + \delta t) = P_0(t) \left[1 - \sum_{j=1}^n a_j \delta t \right] \quad (\text{A.3})$$

where the sum runs over the propensities for all the reactions. Letting δt go to zero implies that

$$\frac{dP_0}{dt} = -P_0 \sum_{j=1}^n a_j \quad (\text{A.4})$$

and so

$$P_0(t) = \mathcal{N} \exp \left(-t \sum_{j=1}^n a_j \right) \quad (\text{A.5})$$

where \mathcal{N} is a normalisation constant that ensures $\int_0^\infty P_0(t) dt = 1$. Thus we have

$$P_i(t) = \mathcal{N} a_i e^{-t \sum_j a_j} \quad (\text{A.6})$$

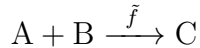
from Eq. A.2 and where \mathcal{N} is chosen so that $\int_0^\infty P_1(t) dt = 1$.

In practice, to choose which reaction to simulate, an n -sided die is rolled with each side corresponding to a reaction and weighted by that reaction's propensity. A second die is then used to determine the time when the reaction occurs by sampling from Eq. A.5. All the chemical species and the time variable are updated following the chosen reaction. For example, if reaction i is chosen then the number of A and B molecules are both decreased by one and the number of C molecules is increased by one, and the propensities of all the reactions are correspondingly recalculated. The process is then repeated, randomly picking both a new reaction and when it happens.

A.1 Mesoscopic and macroscopic rates

The correct way to interpret rate constants is as probabilities per unit time. This interpretation is consistent with the macroscopic one where rates are considered as the reciprocal of the average time taken for the reaction to occur.

For example, consider a system with only one molecule of A and one molecule of B that undergo



where \tilde{f} is the probability of a pair of molecules reacting in unit time. This reaction's propensity will be $a = \tilde{f} \times 1 \times 1$, and, from Eq. A.5, the time taken for the pair to react is given by

$$P_0(t) = ae^{-at} = \tilde{f}e^{-\tilde{f}t} \quad (\text{A.7})$$

which satisfies $\int_0^\infty P_0(t)dt = 1$. We can then calculate the mean time for the reaction

$$\bar{t} = \int_0^\infty t\tilde{f}e^{-\tilde{f}t}dt = \tilde{f}^{-1} \quad (\text{A.8})$$

and so we are able to interpret \tilde{f} too as the reciprocal of the mean time for a pair of molecules to react.

Appendix B Fitting data

Often we want to fit a mathematical model to data, and here we will briefly discuss how to do so. For illustration, we will consider a simple, one-parameter model for a protein A that is degraded at a rate k and we wish to infer k from a data set. The differential equation describing the model is

$$\frac{dA}{dt} = -kA \quad (\text{B.1})$$

and, as well as the parameter k , there is an additional parameter: the initial number of A molecules, denoted A_0 .

We will use a Bayesian approach. In Bayesian probability theory, the probability of an event is interpreted as the degree of belief in that event: the higher the probability, the more confident we are that the event will or has occurred [21].

Inference uses Bayes's rule to update our prior (initial) belief to our posterior belief based on the data that has been observed. In the context of parameter fitting, prior beliefs are typically some range in which we believe the parameter exists, for example, the positive numbers or between some minimum and maximum values. For the parameter k and a data set, D , Bayes's rule is (the symbol $|$ is read as 'given') [21]

$$\begin{aligned} P(k|D) &= \frac{P(D|k)P(k)}{P(D)} \\ &\propto P(D|k)P(k) \end{aligned} \quad (\text{B.2})$$

where \propto means proportional to: we need not be concerned with the denominator because $P(D)$ is independent of the parameter k . The probability $P(k)$ is the prior probability of k ; the

probability $P(D|k)$ is known as the likelihood; and the probability $P(k|D)$ is the posterior probability of k . As we define the prior probability based on our initial knowledge, the likelihood is the only quantity that must be calculated.

For our problem with two unknowns, Bayes's rule becomes

$$P(k, A_0|D) \propto P(D|k, A_0)P(k, A_0) \quad (\text{B.3})$$

and we have to calculate the likelihood given values for k and A_0 consistent with the prior probability.

To calculate the likelihood, we need an explicit model of the measurement error. Usually, the measurement error, ϵ , is assumed to be identically, independently, and normally distributed with a mean of zero and a standard deviation σ , which determines its typical size:

$$P_e(\epsilon) = \frac{\exp\left(\frac{-\epsilon^2}{2\sigma^2}\right)}{\sqrt{2\pi}\sigma} \quad (\text{B.4})$$

If d_i is the data point measured at time t_i and A_i is the corresponding predicted value, found by integrating Eq B.1, then d_i and A_i are related through the measurement error at that time point, ϵ_i :

$$d_i = A_i + \epsilon_i \quad (\text{B.5})$$

or

$$d_i - A_i = \epsilon_i. \quad (\text{B.6})$$

Note that the predicted value A_i depends on the values chosen for the parameters k and A_0 (values are needed to, for example, numerically integrate Eq B.1). Using Eq B.4, we can write

$$\begin{aligned} P(d_i|k, A_0) &= P(d_i|A_i) \\ &= P_e(d_i - A_i) = \frac{\exp\left(\frac{-(d_i - A_i)^2}{2\sigma^2}\right)}{\sqrt{2\pi}\sigma} \end{aligned} \quad (\text{B.7})$$

assuming that the value of σ is known in advance and is part of our prior information.

For the complete likelihood, the error in each data point is assumed to be independent of the error in any other data point, which means that

$$\begin{aligned} P(D|k, A_0) &= P(d_0, \dots, d_n|k, A_0) \\ &= P(d_0, \dots, d_n|A_0, A_1, \dots, A_n) \\ &= P(\epsilon_0, \dots, \epsilon_n) \\ &= P_e(\epsilon_0) \dots P_e(\epsilon_n) \end{aligned} \quad (\text{B.8})$$

where we assume n data points. Using Eq B.7, Eq B.8 is

$$\begin{aligned} P(D|k, A_0) &= \prod_{i=0}^{i=n-1} \frac{\exp\left(\frac{-(d_i - A_i)^2}{2\sigma^2}\right)}{\sqrt{2\pi}\sigma} \\ &= \frac{\exp\left(-\sum_{i=0}^{n-1} \frac{-(d_i - A_i)^2}{2\sigma^2}\right)}{(\sqrt{2\pi}\sigma)^n} \end{aligned} \quad (\text{B.9})$$

which is the complete expression for the likelihood remembering that the A_i are the predictions of the model at times t_i and need to be found typically through numerical integration.

Eq B.9 with the prior distribution, $P(k, A_0)$, and Eq B.3 allows the posterior probability of k and A_0 to be calculated. Figs. 16 and 17 show two example calculations of the posterior probabilities. Although the posterior probability itself is the complete result of the inference, often we wish to give a ‘best-fit’ value for the parameters. These ‘best-fit’ values are the values of the parameters corresponding to the peaks (the modes) of the corresponding posterior distributions and the errors in the inference are given by the width of the posterior distributions at these peaks.

Numerical tricks

When calculating probabilities, often numbers can be small, and there are a few tricks to avoid underflow errors (numbers too small for the computer to store accurately).

First, typically the negative logarithm of the likelihood is calculated. Taking the logarithm of Eq B.9, this ‘energy’, as it is sometimes called in analogy with approaches from physics, is

$$\mathcal{E} = \sum_{i=0}^{n-1} \frac{(d_i - A_i)^2}{2\sigma^2} + n \log(\sqrt{2\pi}) + n \log(\sigma) \quad (\text{B.10})$$

and the most likely values of the parameters are the ones that maximise the likelihood and so minimise the energy. The energy is a sum of squares, which justifies the ‘sum of squares’ approaches that are often used in fitting.

Second, we often wish to find the most probable values of the parameters and so numerically would like to find the values of the parameters that maximise the posterior probability or, equivalently for suitable prior distributions, minimise the energy. Parameter values are typically positive in systems biology, but numerical optimisation schemes may not allow this bound to be imposed. A trick is to transform the parameters

$$k = \exp(\tilde{k}) \quad ; \quad A_0 = \exp(\tilde{A}_0) \quad (\text{B.11})$$

and minimise the energy as a function of \tilde{k} and \tilde{A}_0 . If the optimisation causes either of these transformed parameters to become negative, then k and A_0 are still positive from Eq B.11.

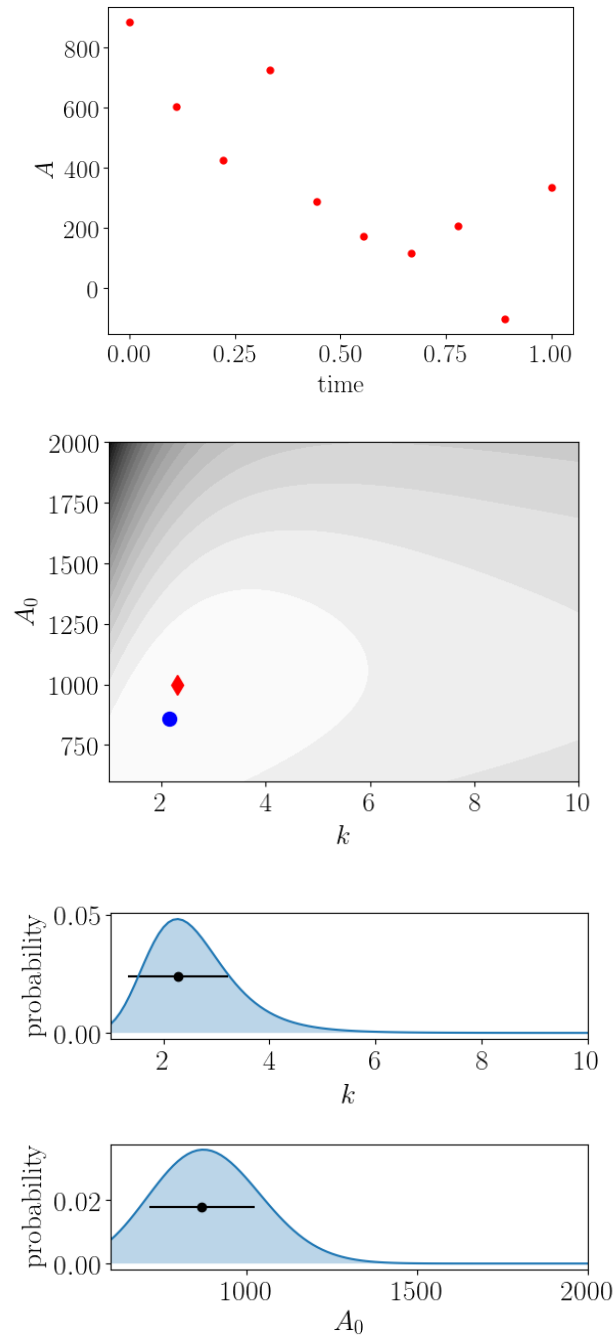


Figure 16: Inference with a few data points ($n = 10$). The data (top), the log posterior probability (middle with the maximum posterior probability marked as a blue dot and the true values of $k = 2.3$ and $A_0 = 1000$ marked with a red diamond), and the posterior probabilities for k and A_0 (bottom) are shown (determined by summing the posterior probability over either A_0 or k values), with the best estimates and their associated errors.

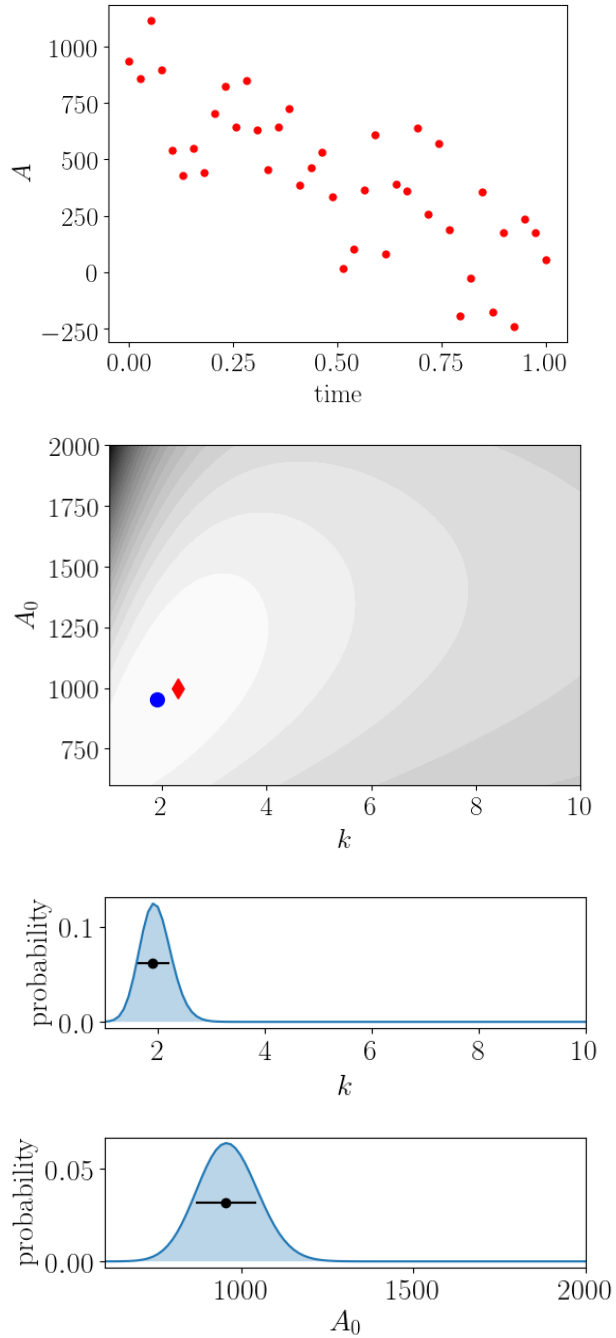


Figure 17: Inference improves with more data ($n = 40$). The data (top), the log posterior probability (middle), and the posterior probabilities for k and A_0 (bottom) are shown. Notice how the posterior probabilities have tightened.

References

- [1] Gillespie DT (1977) Exact stochastic simulation of coupled chemical reactions. *J Phys Chem* 81:2340–2361.
- [2] Dill KA, Bromberg S (2011) *Molecular driving forces* (Garland, New York, New York).
- [3] Nelson P (2004) *Biological physics* (W. H. Freeman, New York, New York).
- [4] Elowitz MB, Surette MG, Wolf PE, Stock JB, Leibler S (1999) Protein mobility in the cytoplasm of escherichia coli. *J Bacteriol* 181:197–203.
- [5] Beard DA, Qian H (2006) *Chemical biophysics: quantitative analysis of chemical systems* (Cambridge University Press, Cambridge, U. K.).
- [6] Monod J, Wyman J, Changeux JP (1965) On the nature of allosteric transitions: a plausible model. *J Mol Biol* 12:88–118.
- [7] Koshland Jr D, Nemethy G, Filmer D (1966) Comparison of experimental binding data and theoretical models in proteins containing subunits. *Biochemistry* 5:365–385.
- [8] Segel LA, Slemrod M (1989) The quasi-steady-state assumption: a case study in perturbation. *SIAM review* 31:446–477.
- [9] Fell D (1996) *Understanding the control of metabolism* (Portland Press, London, U.K.).
- [10] Goldbeter A, Koshland DE (1981) An amplified sensitivity arising from covalent modification in biological systems. *Proc Nat Acad Sci USA* 78:6840–6844.
- [11] Huang CY, Ferrell JE (1996) Ultrasensitivity in the mitogen-activated protein kinase cascade. *Proc Nat Acad Sci* 93:10078–10083.
- [12] Bintu L, *et al.* (2005) Transcriptional regulation by the numbers: models. *Curr Opin Genet Dev* 15:116–124.
- [13] Ferrell Jr JE, *et al.* (2009) Simple, realistic models of complex biological processes: positive feedback and bistability in a cell fate switch and a cell cycle oscillator. *FEBS Lett* 583:3999–4005.
- [14] Strogatz SH (1994) *Nonlinear dynamics and chaos* (Perseus Books, Reading, Massachusetts).
- [15] Tyson JJ, Hong CI, Thron CD, Novak B (1999) A simple model of circadian rhythms based on dimerization and proteolysis of per and tim. *Biophys J* 77:2411–2417.
- [16] Barkai N, Leibler S (2000) Circadian clocks limited by noise. *Nature* 403:267–268.
- [17] Tsai TYC, *et al.* (2008) Robust, tunable biological oscillations from interlinked positive and negative feedback loops. *Science* 321:126–129.
- [18] Vilar JM, Kueh HY, Barkai N, Leibler S (2002) Mechanisms of noise-resistance in genetic oscillators. *Proc Nat Acad Sci USA* 99:5988–5992.

- [19] Krishna S, Semsey S, Jensen M (2009) Frustrated bistability as a means to engineer oscillations in biological systems. *Phys Biol* 6:036009.
- [20] Murray JD (2002) *Mathematical Biology 1: An Introduction* (Springer Verlag).
- [21] Sivia D, Skilling J (2006) *Data analysis: a Bayesian tutorial* (Cambridge University Press, Cambridge, U.K.).